Transportation Research Part B 119 (2019) 79–101

Contents lists available at ScienceDirect

Transportation Research Part B

journal homepage: www.elsevier.com/locate/trb

Distributionally robust optimization of an emergency medical service station location and sizing problem with joint chance constraints

Kanglin Liu, Qiaofeng Li, Zhi-Hai Zhang*

Department of Industrial Engineering, Tsinghua University, Beijing 100084, China

ARTICLE INFO

Article history:
Received 13 July 2018
Revised 25 October 2018
Accepted 26 November 2018

Keywords:
EMS location and sizing problem
Distributionally robust optimization
Joint chance constraints
Mixed integer second-order cone program
Outer approximation

ABSTRACT

An effective Emergency Medical Service (EMS) system can provide medical relief supplies for common emergencies (fire, accident, etc.) or large-scale disasters (earthquake, tsunami, bioterrorism attack, explosion, etc.) and decrease morbidity and mortality dramatically. This paper proposes a distributionally robust model for optimizing the location, number of ambulances and demand assignment in an EMS system by minimizing the expected total cost. The model guarantees that the probability of satisfying the maximum concurrent demand in the whole system is larger than a predetermined reliability level by introducing joint chance constraints and characterizes the expected total cost by moment uncertainty based on a data-driven approach. The model is approximated as a parametric second-order conic representable program. Furthermore, a special case of the model is considered and converted into a standard second-order cone program, which can be efficiently solved with a proposed outer approximation algorithm. Extensive numerical experiments are conducted to illustrate the benefit of the proposed approach. Moreover, a dataset from a real application is also used to demonstrate the application of the data-driven approach.

1. Introduction

An Emergency Medical Service (EMS) is a crucial component of a modern health system. An efficient EMS system makes it possible to rapidly respond to calls, transfer patients, provide timely treatment and save lives the first time emergencies occur to the greatest possible extent (Bélanger et al., 2019). In recent decades, numerous studies concerning EMS systems have been conducted to improve the highly important decision strategies. Trade-offs between efficiency & equity and service quality & cost, as well as the stochasticity inherent in the EMS system, result in challenges to making perfect decisions. With the awareness of humanistic concern and the development of advanced optimization techniques, the EMS location and sizing problem is the top consideration and has received considerable attention, as shown by the numerous review papers in the past few decades (Başar et al., 2012; Ahmadi-Javid et al., 2017; Aringhieri et al., 2017).

Here, we consider an EMS location problem for planning the storage and distribution of medical supplies (ambulances, etc.) to be used in emergencies. In terms of the performance of the EMS system, we mainly concentrate on the availability of ambulances and long-term operational cost. Costly decisions should be taken into consideration due to their long term

* Corresponding author.
E-mail address: zhzhang@tsinghua.edu.cn (Z.-H. Zhang).

https://doi.org/10.1016/j.trb.2018.11.012

implications (Aringhieri et al., 2017). We introduce joint chance constraints to achieve the availability of ambulances, which extends the reliability level of each individual demand site to the entire geographical area.

In order to handle inherent uncertainty in the EMS system, we consider a distributionally robust model (DRM) to make strategic decisions. Distributionally robust optimization (DRO) is an emerging approach that describes random variables through a distributional set with specific properties. Compared with common approaches applied in EMS systems, such as queuing-based paradigms and scenario-based stochastic programming paradigms, the DRO approach has the following advantages: (1) Managers are able to evaluate the worst-case situation by searching through the uncertainty set; and (2) DRO can utilize the data on hand to limit the range of random variables, which alleviates the over-conservatism caused by traditional robust optimization (RO), and is applicable to data-driven problems. Due to its computational tractability and the advantages mentioned above, DRO has been successfully applied to many areas, such as portfolio optimization (Delage and Ye, 2010), lot-sizing problems (Zhang et al., 2016) and appointment scheduling (Mak et al., 2015).

The main contributions of this research include:

1. To the best of our knowledge, this work represents the first time that the EMS station location and sizing problem, which is formulated as a two-stage risk-averse DRM, has been solved by DRO. We can utilize the demand data on hand to estimate the distributional set more precisely and obtain a robust solution by a data-driven approach as well.
2. The proposed program can successfully ensure a high reliability level on the demand sites of the entire geographical area by extending regular individual chance constraints to joint chance constraints. It effectively avoids over-conservative results from the well-known Bonferroni approximation by an iterative algorithm.
3. An outer approximation (OA) algorithm is proposed to solve a special case of the proposed DRM, which can be approximated as a standard second-order cone program (SOCP).
4. Extensive numerical experiments show that the DRM is superior to the traditional scenario-based approach in reliability. Moreover, a dataset from real applications is constructed to demonstrate the application of the proposed DRM. Valuable managerial insights are also observed.

The remainder of the paper is organized as follows. In Section 2, we review the related literature. In Section 3, the problem statement and formulation are presented. Then, the proposed two-stage stochastic program is approximated as a parametric SOCP in Section 4. Section 5 presents the iterative approach to obtain the optimal solution to the parametric SOCP. Moreover, the special case that can be approximated as a standard SOCP is considered, and the OA algorithm is proposed. Extensive numerical experiments are reported in Section 6. Section 7 describes the application of our research to large-scale emergencies. Finally, Section 8 presents the conclusions and outlines future research directions.

2. Literature review

Çelik et al. (2012) pointed out that research problems in the preparedness phase of the relief process, include: facility location and supplies propositioning (Rawls and Turnquist, 2011; Hong et al., 2014), supply distribution (Liberatore et al., 2014; Yuan and Wang, 2009), inventory management (Rottkemper et al., 2011) and restoration of infrastructures network (Nurre et al., 2012; He and Liu, 2012). Despite the unique characteristics of large-scale disasters (tremendous demand and unpredictability), the solutions to the location and sizing optimization in the daily relief process and disaster are generally the same (Jia et al., 2007). The related literature can be classified according to the solution methods. In this paper, we primarily focus on the location and distribution of emergency medical services; thus, a number of papers about EMS are reviewed.

Studies on EMS system design generally fall into two categories: deterministic studies and stochastic studies. Recent studies considering EMS system design as a deterministic problem are often performed in a specific setting. Jia et al. (2007) analyzed the characteristics of large-scale emergencies and proposed tailored location models for EMS system in Los Angeles County. Ndiaye and Alfares (2008) determined the optimal number and locations of primary health units for nomadic population groups by a binary integer program. Scherrer (2008) developed an optimization model to determine the best location and number of new Community Health Centers under several performance metrics. Ares et al. (2016) optimized the locations of Roadside Wellness Centers in Africa based on effectiveness and equity by a column generation approach.

As for EMS design problems considering stochastic factors, the methodologies to address uncertainty used in previous studies can mainly be classified into three categories: the probabilistic paradigm, the stochastic programming paradigm, and the robust counterpart (Aringhieri et al., 2017).

The probabilistic paradigm is generally reflected in the queuing-based approach. Larson (1973) first developed the descriptive hypercube queuing model (HQM) with distinguishable servers in an EMS system by evaluating several point-specific and arc-specific performance measures. Larson (1975) improved the computational tractability of these problems in Larson (1973) by proposing an approximated HQM. Since then, HQM has been widely used in EMS-related research (Galvão and Morabito, 2010). Geroliminis et al. (2009) proposed a Spatial Queuing Model (SQM) examining the coverage and median problems with the consideration of nonidentical service rates among servers and types of responses. Souza et al. (2015) extended the traditional HQM to situations with multiple priority classes and a queue for waiting customers.

Stochastic programming has taken the lead in the EMS location and sizing research. The primary existing literature addresses the stochastic programming paradigm. Two types of stochastic models with different risk preference, which are named as risk-neutral and risk-averse models in academia, are extensively considered in the related research. Most of the existing literature develops risk-neutral stochastic programming models (Salmern and Apte, 2010; Rawls and Turnquist, 2010; Mete and Zabinsky, 2010; Döyen et al., 2011). However, Elçi and Noyan (2018) stated that such models may have the disadvantage of poor performance in the case of rare disasters or undesirable realizations of random data due to the employment of only the expected values and the omission of extreme situations. Therefore, emerging research has begun to focus on risk-averse stochastic programming, following two main approaches: quantitative and qualitative. Quantitative studies consider risk measures in the objective function. For example, Noyan (2012) and Elçi and Noyan (2018) addressed a mean-risk objective based on the well-known risk measure of the conditional value-at-risk (CVaR) in addition to the expectation of the total cost. Dalal and Üster (2018) combined the worst- and average-case considerations in an integrated emergency response network design.

Qualitative works enforce chance constraints to make risk-averse decisions. Chance constraints were first introduced by Charnes et al. (1958) and are defined as

$$\mathbb{P}\{\boldsymbol{A}(\tilde{\boldsymbol{z}}) \geq \boldsymbol{b}(\tilde{\boldsymbol{z}})\} \geq 1-\epsilon, \tag{1}$$

where $\boldsymbol{A}(\tilde{\boldsymbol{z}}) \geq \boldsymbol{b}(\tilde{\boldsymbol{z}})$ represents m linear constraints associated with an $n-$dimensional random vector $\tilde{\boldsymbol{z}}$. The chance constraint ensures that all the m linear constraints are jointly feasible with a probability no less than $1-\epsilon$. The research on chance constraints can be classified into two categories, namely, inequality (1), called an *individual* chance constraint ($m = 1$), and *joint* chance constraints ($m > 1$).

Prékopa (1980) first proposed the idea of developing a stochastic programming model with a probabilistic constraint on the second stage. Beraldi et al. (2004) developed a stochastic programming model with probabilistic constraints for a joint location and dimensioning problem, and solved the problem using a scenario-based approach. Beraldi and Bruni (2009) further built a deterministic equivalent scenario-based counterpart and applied the big-M method to solve the problem. Rawls and Turnquist (2011) extended their earlier research (Rawls and Turnquist, 2010) by adding chance constraints to ensure that the probability of meeting all demand exceeded a predetermined value in all the scenarios. Noyan (2010) introduced integrated chance constraints (ICCs) to EMS system design and obtained convex approximations of the generally non-convex feasible sets defined by chance constraints. Similar to Noyan (2010), Hong et al. (2014) considered a risk-averse two-stage stochastic programming model and specified the conditional-value-at-risk (CVaR) as the risk measure based on a scenario-based approach. Zhang and Li (2015) approximated individual chance constraints as second-order cone constraints in an EMS location problem. Liu et al. (2016) combined the double service coverage standards and multi-vehicle assignments to each demand site to ensure service coverage with the service reliability requirement using chance constraints in two traffic safety metric scenarios. Özgün Elçi et al. (2018) employ individual chance-constrained linear program where the uncertainty (post-disaster demands and transportation network conditions) is limited to the right-hand sides.

Almost all of the above stochastic studies adopted the scenario-based approach for the solution process. Snyder (2007) pointed out two major drawbacks of the scenario-based approach: the difficulty of identifying scenarios and the computational intractability of large-scale problems. A reasonable alternative approach for optimization under uncertainty is robust optimization, which has been successfully applied in the related research. For example, Zhang and Jiang (2014) coped with the uncertain parameters in an EMS design problem by using the robust counterpart method. Ni et al. (2018) proposed a robust min-max model of pre-disaster and post-disaster operations considering three uncertain parameters.

Robust optimization aims to find a solution that performs well in all possible realizations, which may result in over-conservative results. In reality, even though the exact distributions or the enumeration set of random variables cannot be fully recognized, moment information or uncertainty about the distribution itself is usually known (Govindan et al., 2017). DRO considers the moment information or distribution information, and outperforms traditional robust optimization in many areas. Gabrel et al. (2014) divided DRO into two subgroups: robust optimization using moment information and that applied directly to probability distributions. In the first subgroup, the first two moments are often taken into consideration. Scarf et al. (1958) first proposed an inventory model in which only the mean and standard derivation of the demand distribution are known. Becker (2011) addressed a decomposition method for DRO problems with a known mean, covariance and support that recursively derived sub-policies along the projected dimensions. Zymler et al. (2013) developed a tractable and semidefinite program for individual and joint chance constraints given the first two moments of random variables. Mak et al. (2015) applied DRO to the field of appointment scheduling by assuming only the moments information of job durations. Zhang et al. (2016) applied DRO in the context of a two-stage lot-sizing problem based only on mean-covariance information about the distribution. In the second subgroup, uncertainty directly influencing the distributions is taken into account. Delage and Ye (2010) implemented a DRO model that describes uncertainty in accordance with the form of the distribution as well as moments information. Goh and Sim (2010) concentrated on a linear optimization problem under uncertainty and presented a modular framework using expected-value terms to obtain an approximated and flexible solution. Wiesemann et al. (2014) introduced standardized ambiguity sets that can be represented by the many ambiguity sets in recent studies as special cases.

Robust optimization has been extensively applied to obtain valid approximations of individual chance constraints (Ben-Tal and Nemirovski, 1998; Bertsimas and Sim, 2004; Ghaoui et al., 2006; Nemirovski and Shapiro, 2006). Individual chance constraints have been applied to numerous areas, such as closed-loop supply chains (Zhang and Unnikrishnan, 2016) and portfolio optimization (Bonami and Lejeune, 2009). However, studies on approximating joint chance-constrained problems based on robust optimization are far from satisfactory, and only a few related studies have been conducted since 2010 (Chen et al., 2010; Zymler et al., 2013; Hanasusanto et al., 2017).

As seen from the above review, DRO has been successfully applied for many purposes but is rarely used in research on EMS problems. Compared with previous research, our research considers a risk-averse stochastic programming model for the EMS location and sizing problem that simultaneously possesses the following superior properties:

- It considers the worst-case objective function in a quantitative risk-averse way.
- It incorporates joint chance constraints to ensure demand satisfaction in a qualitative risk-averse way.
- It uses DRO to overcome the drawbacks of scenario-based approaches and decreases overconservatism by utilizing the data on hand and advanced DRO methodologies.

3. Problem statement and formulation

We study an EMS network that is composed of multi EMS stations and demand sites. Relief supplies such as ambulances are stored in each EMS station to satisfy uncertain demands from demand sites. Demands at each demand site can be satisfied by at least one EMS station. Two random variables are considered: (daily) demand (Θ_i) and the maximum number of concurrent demands (MNCD) (D_i) occurring at demand site i. The former represents the total number of calling ambulances (in 24 h). The latter denotes the maximum number of emergency calls received within the average time of an emergency task. The goal of our research is to find the optimal EMS station locations and to assign the proper number of ambulances that are used to satisfy a predetermined reliability level associated with the entire EMS network with the objective of minimizing the total cost, which includes location cost, transportation cost, and the cost to maintain and purchase the ambulances.

We propose the EMS location and sizing problem as a two-stage DRM. The notation used throughout the paper is summarized as follows.

Parameters:

I	set of demand sites, indexed by i
J	set of candidate EMS stations, indexed by j
I_j	set of demand sites that can be covered by EMS station j, i.e., $I_j = \{i \in I \mid c_{ij} \le T\}$
J_i	set of candidate EMS stations that can cover demand site i, i.e., $J_i = \{j \in J \mid c_{ij} \le T\}$
T	the maximal length of time required for the service trip
f_j	(daily) construction cost at EMS station j
a_j	(daily) maintenance and purchase costs per ambulance at EMS station j
c_{ij}	distance between demand site i and EMS station j
β	unit transportation cost
Θ_i	random variable that represents (daily) demand at demand site i
D_i	random variable that represents MNCD occurring at demand site i
α	the reliability level of the EMS system for the entire geographical area
M	a sufficiently large positive number

Decision variables:

X_{ij}	percentage of demand at demand site i served by EMS station j
Y_j	1, if an EMS station is constructed at candidate EMS station j; 0 otherwise
N_j	number of ambulances at EMS station j

Note that we use boldface letters to denote vectors or matrices.

A joint chance constraint is introduced to ensure the reliability of the EMS system for the entire geographical area. This constraint is an extension of individual chance constraints, which are extensively used in research on EMS location problems (Ball and Lin, 1993; Özgün Elçi et al., 2018), though they cannot guarantee system reliability. Chance constraints are capable of quantifying unsatisfied demand by a precise service level, whereas traditional robust optimization, such as Zhang and Jiang (2014), roughly characterizes the uncertainty set by exogenous safety parameters. Note that the our research differs from the most relevant work of Zhang and Li (2015) in the following three aspects:

- We employ joint change constraints instead of using standard individual chance constraints. The extension not only dramatically improves system reliability in practice but also establishes the relationship between joint and individual chance constraints through several unique properties.
- We quantitatively incorporate a risk-averse, rather than risk-neutral, objective. Additionally, data are utilized to estimate the distributional set less conservatively.
- We propose an outer approximation algorithm to evade computational intractability when random variables are limited in a specified ellipsoid. By contrast, Zhang and Li (2015) solved their problem with an off-the-shelf solver.

The joint chance constraint associated with MNCD and the number of ambulances is formulated as

$$\mathbb{P}\left\{\sum_{i \in I_j} D_i X_{ij} \le N_j, \forall j \in J\right\} \ge \alpha. \tag{2}$$

The EMS location and sizing problem is formulated as a two-stage risk-averse DRM with joint chance constraints (2), which is expressed as follows.

$$P: \min \left(\sum_{j\in J} f_j Y_j + \sum_{j\in J} a_j N_j + \sup_{\substack{F\in\mathcal{F}\\ G\in\mathcal{G}}} \mathbb{E}_{F,G}[g(\boldsymbol{Y}, \boldsymbol{N}, \boldsymbol{\Theta}, \boldsymbol{D})] \right), \tag{3}$$

$$s.t.\ N_j \le MY_j, \forall j \in J, \tag{4}$$

$$Y_j \in \{0, 1\}, \forall j \in J, \tag{5}$$

$$N_j \in \mathbb{Z}^+, \forall j \in J. \tag{6}$$

The purpose of objective function (3) is to minimize the supremum of the expected total cost by restricting the distributions of the random variables $\boldsymbol{\Theta}$ and $\boldsymbol{D}$ to specified distributional sets $\mathcal{F}$ and $\mathcal{G}$. The total cost is the sum of the EMS station construction costs, the maintenance and purchase costs for ambulances and the transportation cost. Note that $g(\boldsymbol{Y}, \boldsymbol{N}, \theta, \boldsymbol{d})$ is the second-stage cost for given $\boldsymbol{Y}$, $\boldsymbol{N}$, $\boldsymbol{\Theta} = \boldsymbol{\theta}$ and $\boldsymbol{D} = \boldsymbol{d}$. Suppose F and G are the joint probability distribution functions of distributional sets $\mathcal{F}$ and $\mathcal{G}$, where $\mathcal{F}$ and $\mathcal{G}$ are composed of a series of distributions with specific properties for $\boldsymbol{\Theta}$ and $\boldsymbol{D}$, respectively. We assume that F and G are unknown but belong to the predefined distributional sets $\mathcal{F}$ and $\mathcal{G}$. Constraint (4) implies that ambulances can only be assigned to open EMS stations. Constraints (5) and (6) are standard binary and non-negative integral constraints.

The second-stage cost function is given as follows:

$$g(\boldsymbol{Y}, \boldsymbol{N}, \boldsymbol{\theta}, \boldsymbol{d}) = \min\ \beta \sum_{i\in I} \left(\theta_i \sum_{j\in J} c_{ij} X_{ij} \right), \tag{7}$$

$$s.t.\ \sum_{j\in J_i} X_{ij} = 1, \forall i \in I, \tag{8}$$

$$X_{ij} \le Y_j, \forall i \in I, \forall j \in J, \tag{9}$$

$$\mathbb{P}\left\{ \sum_{i\in I_j} d_i X_{ij} \le N_j, \forall j \in J \right\} \ge \alpha, \tag{10}$$

$$0 \le X_{ij} \le 1. \tag{11}$$

Objective function (7) minimizes the total transportation cost. Constraint (8) requires that the demand of each site is completely assigned to the associated EMS stations. Constraint (9) indicates that demand sites can only be assigned to an open EMS station. Constraint (10) is the joint chance constraint. Constraint (11) stands for the range of X_{ij}.

4. Reformulation

Since the proposed model with joint chance constraints is nonconvex and computationally intractable, we reformulate it into a parametric second-order cone program (SOCP) by estimating the expected daily demand via a data-driven approach based on DRO (Delage and Ye, 2010) and defining MNCD in an ellipsoid set with a known mean and covariance (Zhang and Jiang, 2014). The reason that we use the two different approaches for the two random variables is that daily demand is relatively stable because peak values can be averaged throughout considerable amounts of historical data, while the MNCD may exhibit violent fluctuations due to the existence of unforeseeable emergencies or disasters within a given time period.

4.1. Objective function

Function (7) shows that when the construction decision $\boldsymbol{Y}$ and the number of ambulances $\boldsymbol{N}$ are fixed, optimal solutions of the second-stage problem only depend on the unit transportation cost (β), distance parameters (c_{ij}) and (daily) demand at demand site i (θ_i). Since objective function (7) is linear in $\boldsymbol{\theta}$, the expectation of $g(\boldsymbol{Y}, \boldsymbol{N}, \boldsymbol{\theta}, \boldsymbol{d})$ is only determined by the (daily) expected demand. Thus, considering the first moment uncertainty of (daily) demand $\boldsymbol{\Theta}$ is sufficient to establish the uncertain performance within the distributional set $\mathcal{F}$. In this study, we assume that the first moment $\mathbb{E}_F[\boldsymbol{\Theta}]$ is subject to an ellipsoid set with an estimated mean $\boldsymbol{\mu} \in \mathbb{R}^T$ and an estimated covariance matrix $\boldsymbol{\Sigma} \succeq 0$, which can be depicted by the following distributional set:

$$\mathcal{F} = \left\{ F : (\mathbb{E}_F[\boldsymbol{\Theta}] - \boldsymbol{\mu})^T \boldsymbol{\Sigma}^{-1} (\mathbb{E}_F[\boldsymbol{\Theta}] - \boldsymbol{\mu}) \le \epsilon^2 \right\}, \tag{12}$$

where, $\epsilon > 0$ controls the size of $\mathcal{F}$. The selection of ϵ relies on the accuracy of estimating the first moment.

The data-driven approach proposed by Delage and Ye (2010) is applied to determine the value of ϵ in (12) on the basis of a set of M independent samples $\{\theta^i\}_{i=1}^M$ of $\boldsymbol{\Theta}$. Suppose the mean and covariance matrix of $\boldsymbol{\Theta}$ is $\boldsymbol{\mu_0}$ and $\boldsymbol{\Sigma}_0$. If there exists an $R \ge 0$ and a $\delta > 0$ such that $\mathbb{P}\{(\boldsymbol{\Theta} - \boldsymbol{\mu_0})^T \boldsymbol{\Sigma_0}^{-1} (\boldsymbol{\Theta} - \boldsymbol{\mu_0}) \le R^2\} = 1$, then with a probability greater than $1 - \delta$, we have

$$(\boldsymbol{\mu_0} - \hat{\boldsymbol{\mu}})^T \boldsymbol{\Sigma_0}^{-1} (\boldsymbol{\mu_0} - \hat{\boldsymbol{\mu}}) \le \eta(\delta), \tag{13}$$

where $\hat{\boldsymbol{\mu}} = (1/M) \sum_{i=1}^M \theta^i$ and $\eta(\delta) = (R^2/M)[2 + \sqrt{2 \ln(1/\delta)}]^2$.

Proposition 4.1. *Problem P is reformulated as the following program,*

$$\min_{r, \boldsymbol{q}, \boldsymbol{X}, \boldsymbol{Y}, \boldsymbol{N}} \beta(\epsilon r + \boldsymbol{\mu}^T \boldsymbol{q}) + \sum_{j \in J} \left\{ f_j Y_j + a_j N_j \right\}, \tag{14}$$

$$s.t.\ q_i = \sum_{j \in J_i} c_{ij} X_{ij}, \forall i, \tag{15}$$

$$\|\boldsymbol{\Sigma}^{\frac{1}{2}} \boldsymbol{q}\| \le r, \tag{16}$$

$$r \ge 0, q \ge 0, \tag{17}$$

$$(4) \sim (6), (8) \sim (11),$$

where, r and $\boldsymbol{q}$ are auxiliary decision variables.

Proof. Please refer to Appendix A. □

4.2. Chance constraints

The distribution function G of $\boldsymbol{D}$ is constrained in the following ellipsoid uncertainty set:

$$\mathcal{G} = \left\{ G : \begin{array}{l} (\boldsymbol{D} - \boldsymbol{u})^T \boldsymbol{\Gamma}^{-1} (\boldsymbol{D} - \boldsymbol{u}) \le Q^2 \\ \mathbb{E}_G(\boldsymbol{D}) = \boldsymbol{u} \\ \mathbb{E}_G(\boldsymbol{D}^2) = \boldsymbol{u}^T \boldsymbol{u} + \boldsymbol{\Gamma} \end{array} \right\}, \tag{18}$$

where, $Q > 0$ controls the size of $\mathcal{G}$. Although an alternative, box uncertainly set, is well-known in the related research as well, it is not considered because of its over-conservationism (Baron et al., 2011).

We firstly introduce a conic transformation of individual chance constraints in Proposition 4.4. And then, the transformation is extended to a joint chance-constrained framework.

Define $\nu(N_j, \boldsymbol{X}_j) = \sum_{i \in I_j} d_i X_{ij} - N_j = \boldsymbol{X}_j^T \boldsymbol{d} - N_j$. The conic transformation for individual chance constraints are based on the upper bound of $\mathbb{E}(\nu(N_j, \boldsymbol{X}_j)^+)$, which is obtained in Lemma 4.2. Moreover, the upper bound is a subadditive function proved in Lemma 4.3.

Lemma 4.2. *Suppose $\boldsymbol{u}$ and $\boldsymbol{\Gamma}$ are the mean and covariance matrix of random variable $\boldsymbol{d}$ respectively, $\pi(N_j, \boldsymbol{X}_j)$ is an upper bound of $\mathbb{E}(\nu(N_j, \boldsymbol{X}_j)^+)$, where,*

$$\pi(N_j, \boldsymbol{X}_j) = \frac{1}{2}(\boldsymbol{X}_j^T \boldsymbol{u} - N_j) + \frac{1}{2}\sqrt{(\boldsymbol{X}_j^T \boldsymbol{u} - N_j)^2 + \boldsymbol{X}_j^T \boldsymbol{\Gamma} \boldsymbol{X}_j}. \tag{19}$$

Proof. Because of the relation $w^+ = (w + |w|)/2$, then, $\mathbb{E}\left[\nu(N_j, \boldsymbol{X}_j)^+\right] = \frac{1}{2}\mathbb{E}\left(\nu(N_j, \boldsymbol{X}_j) + \left|\nu(N_j, \boldsymbol{X}_j)\right|\right)$. For a convex function $\psi(\cdot)$, Jensen's inequality $\psi[\mathbb{E}(X)] \le \mathbb{E}[\psi(X)]$ holds; thus,

$$\begin{aligned}
\left[\mathbb{E}\left|\nu(N_j, \boldsymbol{X}_j)\right|\right]^2 &\le \mathbb{E}\left[\left|\nu(N_j, \boldsymbol{X}_j)\right|^2\right] = \mathbb{E}\left[\left|\boldsymbol{X}_j^T \boldsymbol{d} - N_j\right|^2\right], \\
&= \mathbb{E}\left[\left(\boldsymbol{X}_j^T \boldsymbol{d}\right)^2 + N_j^2 - 2N_j \boldsymbol{X}_j^T \boldsymbol{d}\right], \\
&= N_j^2 + \mathbb{E}\left[\left(\boldsymbol{X}_j^T \boldsymbol{d}\right)^2\right] - 2N_j \boldsymbol{X}_j^T \mathbb{E}(\boldsymbol{d}), \\
&= \left[\boldsymbol{X}_j^T \mathbb{E}(\boldsymbol{d})\right]^2 + \boldsymbol{X}_j^T \boldsymbol{\Gamma} \boldsymbol{X}_j + N_j^2 - 2N_j \boldsymbol{X}_j^T \mathbb{E}(\boldsymbol{d}), \\
&= \left(\boldsymbol{X}_j^T \boldsymbol{u}\right)^2 + \boldsymbol{X}_j^T \boldsymbol{\Gamma} \boldsymbol{X}_j + N_j^2 - 2N_j \boldsymbol{X}_j^T \boldsymbol{u},
\end{aligned}$$

$$= (\boldsymbol{X}_j^T\boldsymbol{u} - N_j)^2 + \boldsymbol{X}_j^T\boldsymbol{\Gamma}\boldsymbol{X}_j.$$

The first inequality holds because function $\psi(x) = x^2$ is convex. Therefore, $\mathbb{E}\left[\nu(N_j, \boldsymbol{X}_j)^+\right] \le \frac{1}{2}(\boldsymbol{X}_j^T\boldsymbol{u} - N_j) + \frac{1}{2}\sqrt{(\boldsymbol{X}_j^T\boldsymbol{u} - N_j)^2 + \boldsymbol{X}_j^T\boldsymbol{\Gamma}\boldsymbol{X}_j} = \pi(N_j, \boldsymbol{X}_j)$. □

Lemma 4.3. *$\pi(N, \boldsymbol{X})$ is a subadditive function, i.e., $\pi(N_1, \boldsymbol{X}_1) + \pi(N_2, \boldsymbol{X}_2) \ge \pi(N_1 + N_2, \boldsymbol{X}_1 + \boldsymbol{X}_2)$.*

Proof. Suppose $S = \boldsymbol{X}^T\boldsymbol{u} - N$, $\boldsymbol{U} = (S, \boldsymbol{X})$, and $\boldsymbol{\Gamma}_1 = \left(\begin{array}{c|ccc} 1 & 0 & \cdots & 0 \\ \vdots & & & \\ 0 & & \boldsymbol{\Gamma} & \end{array}\right)$, where, $\boldsymbol{\Gamma}_1$ is a positive semidefinite matrix. Then, $\sqrt{(\boldsymbol{X}^T\boldsymbol{u} - N)^2 + \boldsymbol{X}^T\boldsymbol{\Gamma}\boldsymbol{X}} = \sqrt{S^2 + \boldsymbol{X}^T\boldsymbol{\Gamma}\boldsymbol{X}} = \sqrt{\boldsymbol{U}^T\boldsymbol{\Gamma}_1\boldsymbol{U}} = \left\|\boldsymbol{\Gamma}_1^{\frac{1}{2}}\boldsymbol{U}\right\|$, and $||\cdot||$ is the Euclidean norm. Because norm is a subadditive function, i.e., $||A|| + ||B|| \ge ||A + B||$, then $\left\|\boldsymbol{\Gamma}_1^{\frac{1}{2}}\boldsymbol{U}_1\right\| + \left\|\boldsymbol{\Gamma}_1^{\frac{1}{2}}\boldsymbol{U}_2\right\| \ge \left\|\boldsymbol{\Gamma}_1^{\frac{1}{2}}(\boldsymbol{U}_1 + \boldsymbol{U}_2)\right\|$. Thus, proved. □

After obtaining the upper bound of $\mathbb{E}(N_j, \boldsymbol{X}_j)$, the conic transformation for individual chance constraints is summarized in Proposition 4.4.

Proposition 4.4. *A conic transformation of individual chance constraints*

$$\mathbb{P}\left\{\sum_{i \in I_j} d_i X_{ij} - N_j \le 0\right\} \ge 1 - \varepsilon, \forall j \in J, \tag{20}$$

is as follows:

$$\boldsymbol{X}_j^T\boldsymbol{u} - N_j + \sqrt{\frac{1-\varepsilon}{\varepsilon}}\sqrt{\boldsymbol{X}_j^T\boldsymbol{\Gamma}\boldsymbol{X}_j} \le 0, \forall j \in J, \tag{21}$$

where, $\varepsilon = 1 - \alpha$.

Proof. By convention, each individual chance constraint is approximated by the CVaR measure (Ben-Tal and Teboulle, 1986), which provides computational tractability through convex approximations. Rockafellar and Uryasev (2010) popularized the approach according to the definition of CVaR, $\varrho_{1-\varpi}(\cdot)$, as follows:

$$\varrho_{1-\varpi}(\tilde{\nu}) \triangleq \min_{\iota}\left\{\iota + \frac{1}{\varpi}\mathbb{E}[(\tilde{\nu} - \iota)^+]\right\}, \tag{22}$$

where $\tilde{\nu}$ is a random variable and $\varpi \in \{0, 1\}$ is a desired safety factor that is near to zero. CVaR represents the conditional expectation of loss above the $1 - \varpi$ quantile of the distribution. It is well known that CVaR constraint $\varrho_{1-\varpi}[y(\tilde{\boldsymbol{z}})] \le 0$ is the tightest convex approximation to the individual chance constraint $\mathbb{P}\{y(\tilde{\boldsymbol{z}}) \le 0\} \ge 1 - \varpi$, where $y(\tilde{\boldsymbol{z}})$ is affinely dependent on random vector $\tilde{\boldsymbol{z}}$ (Nemirovski and Shapiro, 2006; Chen et al., 2010). Thus,

$$\min_{\iota}\left\{\iota + \frac{1}{\varepsilon}\mathbb{E}\left[\left(\sum_{i \in I_j} d_i X_{ij} - N_j - \iota\right)^+\right]\right\} \le 0.$$

is sufficient to imply (20).

Since the closed-from solution of $\mathbb{E}\left[\left(\sum_{i \in I_j} d_i X_{ij} - N_j - \iota\right)^+\right]$ is still computationally intractable, utilizing the upper bound of $\mathbb{E}[(\cdot)^+]$ in Lemma 4.2, we obtain,

$$\begin{aligned}
\varrho_{1-\varepsilon}[\nu(N_j, \boldsymbol{X}_j)] &\le \min_{\iota}\left(\iota + \frac{\pi(N_j + \iota, \boldsymbol{X}_j)}{\varepsilon}\right) \\
&= \min_{\iota}\left(\iota + \frac{\boldsymbol{X}_j^T\boldsymbol{u} - N_j - \iota}{2\varepsilon} + \frac{\sqrt{(\boldsymbol{X}_j^T\boldsymbol{u} - N_j - \iota)^2 + \boldsymbol{X}_j^T\boldsymbol{\Gamma}\boldsymbol{X}_j}}{2\varepsilon}\right) \\
&= \boldsymbol{X}_j^T\boldsymbol{u} - N_j + \sqrt{\frac{1-\varepsilon}{\varepsilon}}\sqrt{\boldsymbol{X}_j^T\boldsymbol{\Gamma}\boldsymbol{X}_j},
\end{aligned} \tag{23}$$

where the last equality holds when $\iota^* = \frac{(1-2\varepsilon)\sqrt{\boldsymbol{X}_j^T\boldsymbol{\Gamma}\boldsymbol{X}_j}}{2\sqrt{\varepsilon(1-\varepsilon)}} + \boldsymbol{X}_j^T\boldsymbol{u} - N_j$. Thus, inequality (21) is a valid conic transformation of individual chance constraints (20). □

The conic transformation of individual chance constraints described in Proposition 4.4 can be extended to a program with joint chance constraints.

Constraint (10) is equivalent to $\mathbb{P}\left(\bigcup_{j\in J}\left\{\sum_{i\in I_j} d_i X_{ij} > N_j\right\}\right) \le \varepsilon$. A well-known approximation for decomposing joint chance constraints to individual ones is based on Bonferroni's inequality, which implies the following:

$$\mathbb{P}\left(\bigcup_{j\in J}\left\{\sum_{i\in I_j} d_i X_{ij} - N_j > 0\right\}\right) \le \sum_{j\in J}\left[\mathbb{P}\left(\sum_{i\in I_j} d_i X_{ij} - N_j > 0\right)\right] \le \varepsilon. \tag{24}$$

Hence, the joint chance constraints can be decomposed into several individual ones, i.e.,

$$\mathbb{P}\left(\sum_{i\in I_j} d_i X_{ij} - N_j > 0\right) \le \varepsilon_j, \forall j, \Rightarrow \mathbb{P}\left(\sum_{i\in I_j} d_i X_{ij} - N_j \le 0\right) \ge 1 - \varepsilon_j, \forall j, \tag{25}$$

where $\sum_{j\in J}\varepsilon_j = \varepsilon$. Since the only difference between individual chance constraint (20) and the result of the Bonferroni approximation (25) is the value of ε and ε_i, the joint chance constraint (10) can be approximated to (21). Nevertheless, it is intractable to choose a proper value of ε_i. Therefore, Nemirovski and Shapiro (2006) and Chen et al. (2007) directly supposed $\varepsilon_i = \varepsilon/|J|$, which results in an over-conservative approximation.

Define set $\mathcal{W}$ as containing the support of the primitive uncertainty of MNCD ($\boldsymbol{D}$). Following the approximation approach proposed by Chen et al. (2010),we propose a parametric SOCP in Proposition 4.5 to optimize the EMS location and sizing problem, where two parameters, the set $\mathcal{J}$ (a subset of $\mathcal{W}$) and the constants $\lambda_j > 0, \forall j \in \mathcal{J}$, are introduced in (26) and (27). λ_j is a positive scaling parameter. Its value does not affect the feasible region of joint chance constraint (2) but can improve the approximation (Zymler et al., 2013). The conic transformation for individual chance constraints is added $|J|$ times for each demand site j in the standard Bonferroni approximation, i.e., $\mathbb{P}\left\{\boldsymbol{X}_j^T\boldsymbol{d} - N_j\right\} \ge 0, \forall j$, while only one conic transformation for the maximum value with fixed λ and $\mathcal{J}$ is applied, i.e., $\mathbb{P}\left\{\max_{j\in\mathcal{J}}\left(\lambda_j\left[\boldsymbol{X}_j^T\boldsymbol{d} - N_j\right]\right) \ge 0\right\}$, which is defined in Proposition 4.5.

Proposition 4.5. *Define*

$$\Upsilon(\boldsymbol{N},\boldsymbol{X},\boldsymbol{\lambda},\mathcal{J}) \triangleq \min_{w_0,\boldsymbol{w}}\left\{\min_{\iota}\left[\iota + \frac{\pi(w_0+\iota,\boldsymbol{w})}{\varepsilon}\right] + \frac{1}{\varepsilon}\left[\sum_{j\in\mathcal{J}}\pi\left(\lambda_j N_j - w_0, \lambda_j\boldsymbol{X}_j - \boldsymbol{w}\right)\right]\right\};$$

then,

$$\Upsilon(\boldsymbol{N},\boldsymbol{X},\boldsymbol{\lambda},\mathcal{J}) \le 0 \tag{26}$$

and

$$\max_{j\in\mathcal{W}\setminus\mathcal{J}}\left[\boldsymbol{X}_j^T\boldsymbol{d} - N_j\right] \le 0 \tag{27}$$

are sufficient to guarantee chance constraint (10).

Proof. Similar to Theorem 3.1. of Chen et al. (2010). Please refer to Appendix B for more details. □

Define the upper bound of $\varrho_{1-\varepsilon}[\nu(N_j,\boldsymbol{X}_j)]$ as $\phi_{1-\varepsilon}(N_j,\boldsymbol{X}_j)$ which equals to $\phi_{1-\varepsilon}(N_j,\boldsymbol{X}_j) = \boldsymbol{X}_j^T\boldsymbol{u} - N_j + \sqrt{\frac{1-\varepsilon}{\varepsilon}}\sqrt{\boldsymbol{X}_j^T\boldsymbol{\Gamma}\boldsymbol{X}_j}$ based on (23). Inequalities (26) and (27) in Proposition 4.5 constitute the conic quadric approximation for the joint chance constraint (10). By introducing two auxiliary variables, s_0 and s_j, inequality (26) is equivalent to the following three constraints:

$$s_0 + \frac{1}{\varepsilon}\sum_{j\in\mathcal{J}} s_j \le 0, \tag{28}$$

$$\phi_{1-\varepsilon}(w_0,\boldsymbol{w}) \le s_0, \tag{29}$$

$$\pi\left(\lambda_j N_j - w_0, \lambda_j\boldsymbol{X}_j - \boldsymbol{w}\right) \le s_j, \forall j \in \mathcal{J}, \tag{30}$$

Moreover, recall that MNCD ($\boldsymbol{D}$) belongs to distributional set (18) and based on Theorem 3 of Chen and Sim (2009), we obtain,

$$\max\left[\boldsymbol{X}_j^T\boldsymbol{d} - N_j\right] = \boldsymbol{X}_j^T\boldsymbol{u} - N_j + Q\sqrt{\boldsymbol{X}_j^T\boldsymbol{\Gamma}\boldsymbol{X}_j}, \tag{31}$$

then, inequality (27) is expressed as $\boldsymbol{X}_j^T\boldsymbol{u} - N_j + Q\sqrt{\boldsymbol{X}_j^T\boldsymbol{\Gamma}\boldsymbol{X}_j} \le 0$.

To sum up, problem P is reformulated as the following SOCP with parameters λ_j and $\mathcal{J}$ (RP-SOCP henceforth):

$$\text{RP-SOCP}: \min \ \beta(\epsilon r + \boldsymbol{\mu}^T \boldsymbol{q}) + \sum_{j \in J} \left\{ f_j Y_j + a_j N_j \right\}, \tag{32}$$

$$s.t. \ \boldsymbol{X}_j^T \boldsymbol{u} - N_j + Q\sqrt{\boldsymbol{X}_j^T \boldsymbol{\Gamma} \boldsymbol{X}_j} \le 0, \forall j \in \mathcal{W} \setminus \mathcal{J}, \tag{33}$$
$$(5), (6), (8), (9), (11), (15), (16), (17), (28), (29), (30).$$

4.3. Properties associated with RP-SOCP

The following theorem illustrates the benefit of the parametric SOCP approximation for joint chance constraints relative to its individual counterpart in terms of system reliability.

Theorem 4.6. *Inequalities (28)–(30) dominate inequality (21)* $\forall j \in \mathcal{J}$.

Proof. Because (28)–(30) are equivalent to $\Upsilon(\boldsymbol{N}, \boldsymbol{X}, \boldsymbol{\lambda}, \mathcal{J}) \le 0$, then,

$$\begin{aligned}
0 \ &\ge \ \min_{\iota, \boldsymbol{w}, w_0} \left\{ \iota + \frac{1}{\varepsilon}\left[\pi(w_0 + \iota, \boldsymbol{w}) + \sum_{j \in \mathcal{W}} \pi(\lambda_j N_j - w_0, \lambda_j \boldsymbol{X}_j - \boldsymbol{w}) \right] \right\}, \\
&\ge \ \min_{\iota, \boldsymbol{w}, w_0} \left\{ \iota + \frac{1}{\varepsilon}\left[\pi(w_0 + \iota, \boldsymbol{w}) + \pi(\lambda_j N_j - w_0, \lambda_j \boldsymbol{X}_j - \boldsymbol{w}) \right] \right\}, \\
&\ge \ \min_{\iota} \left\{ \iota + \frac{1}{\varepsilon}\left[\pi(\lambda_j N_j + \iota, \lambda_j \boldsymbol{X}_j) \right] \right\}, \\
&\overset{\lambda_j = 1}{=} \ \min_{\iota} \left\{ \iota + \frac{1}{\varepsilon}\left[\pi(N_j + \iota, \boldsymbol{X}_j) \right] \right\}, \\
&= \ \boldsymbol{X}_j^T \boldsymbol{u} - N_j + \sqrt{\frac{1-\varepsilon}{\varepsilon}} \sqrt{\boldsymbol{X}_j^T \boldsymbol{\Gamma} \boldsymbol{X}_j},
\end{aligned}$$

in which, the first inequality is valid through the definition of $\Upsilon(\boldsymbol{N}, \boldsymbol{X}, \boldsymbol{\lambda}, \mathcal{J})$ in Proposition 4.5; the second inequality holds by selecting $\pi(\lambda_j N_j - w_0, \lambda_j \boldsymbol{X}_j - \boldsymbol{w})$ for facility j out of the summation; the third inequality is based on the subadditivity of $\pi(\cdot, \ \cdot)$ in Lemma 4.3; the last two equalities are established by supposing $\lambda_j = 1$ and (23), respectively. □

In our specified setting of an ellipsoid uncertainty set, RP-SOCP harbors the following superior properties, Proposition 4.7, Lemma 4.8 and Theorem 4.9, with respect to the radius Q.

Proposition 4.7. *When* $Q \le \sqrt{\frac{1-\varepsilon}{\varepsilon}}$, *RP-SOCP obtains its optimal solution with* $\mathcal{J} = \emptyset$.

Proof. We prove this proposition by contradiction. Without loss of generality, suppose there exists an arbitrary $j^\circ \in \mathcal{J}$ in the optimal solution such that $\mathcal{J} \ne \emptyset$. For all $j \in \mathcal{J}$, we need to ensure $\Upsilon(\boldsymbol{N}, \boldsymbol{X}, \boldsymbol{\lambda}, \mathcal{J}) \le 0$. Meanwhile,

$$\begin{aligned}
0 \ge \Upsilon(\boldsymbol{N}, \boldsymbol{X}, \boldsymbol{\lambda}, j^\circ) &\ge \boldsymbol{X}_{j^\circ}^T \boldsymbol{u} - N_{j^\circ} + \sqrt{\frac{1-\varepsilon}{\varepsilon}} \sqrt{\boldsymbol{X}_{j^\circ}^T \boldsymbol{\Gamma} \boldsymbol{X}_{j^\circ}}, \\
&\ge \boldsymbol{X}_{j^\circ}^T \boldsymbol{u} - N_{j^\circ} + Q\sqrt{\boldsymbol{X}_{j^\circ}^T \boldsymbol{\Gamma} \boldsymbol{X}_{j^\circ}},
\end{aligned}$$

where the first inequality holds according to Theorem 4.6, and the second inequality stands as a result of $Q \le \sqrt{\frac{1-\varepsilon}{\varepsilon}}$. Therefore, $\boldsymbol{X}_{j^\circ}^T \boldsymbol{u} - N_{j^\circ} + Q\sqrt{\boldsymbol{X}_{j^\circ}^T \boldsymbol{\Gamma} \boldsymbol{X}_{j^\circ}} \le 0$ is less conservative than $\Upsilon(\boldsymbol{N}, \boldsymbol{X}, \boldsymbol{\lambda}, j^\circ) \le 0$. That is, a better solution is obtained if $j^\circ \in \mathcal{W} \setminus \mathcal{J}$ (i.e., $j^\circ \notin \mathcal{J}$). This results in a contradiction since the result obtained when $\mathcal{J} \ne \emptyset$ is not optimal, thus completing the proof. □

Consequently, Proposition 4.7 reveals that RP-SOCP is equivalent to a standard SOCP (Zhang et al., 2015) that is unrelated to λ_j and $\mathcal{J}$ when $Q \le \sqrt{\frac{1-\varepsilon}{\varepsilon}}$. Moreover, this SOCP can be efficiently solved with a customized OA algorithm proposed in the following section.

Lemma 4.8. *When* $Q \le \sqrt{\frac{1-\varepsilon}{\varepsilon}}$, *RP-SOCP is equivalent to the following program RP-1.*

$$\begin{aligned}
\text{RP-1}: \min \ & \beta(\epsilon r + \boldsymbol{\mu}^T \boldsymbol{q}) + \sum_{j \in J} \left\{ f_j Y_j + a_j N_j \right\}, \\
s.t. \ & (5), (6), (8), (9), (11), (15), (16), (17), (33).
\end{aligned} \tag{34}$$

Algorithm 1 Algorithm to solve RP-SOCP.

Input: TC: objective function of problem RP-SOCP with the initial value $TC^1 = 0$.
$\mathcal{H}(\boldsymbol{X}, \boldsymbol{N})$: a subset of set $\mathcal{W}$ with the initial value $\mathcal{H}^1(\boldsymbol{X}, \boldsymbol{N}) = \mathcal{W}$.
$\boldsymbol{\lambda}$: a set of constants with the initial value $\lambda_j^1 = 1/|J|, \forall j \in \mathcal{H}^1(\boldsymbol{X}, \boldsymbol{N})$.
τ: a small number.
K: the maximal number of iterations.
Procedure:
for $k = 1 : K$ **do**
  Solve model RP-SOCP with input $\boldsymbol{\lambda}^k$, $\mathcal{H}^k(\boldsymbol{X}, \boldsymbol{N})$. Obtain optimal solution ($\boldsymbol{Y}^*$, $\boldsymbol{X}^*$, $\boldsymbol{N}^*$) and the minimal objective TC^*. Update ($\boldsymbol{Y}^k$, $\boldsymbol{X}^k$, $\boldsymbol{N}^k$)=($\boldsymbol{Y}^*$, $\boldsymbol{X}^*$, $\boldsymbol{N}^*$) and $TC^{k+1} = TC^*$.
  if $TC^{k+1} - TC^k \leq \tau$ or $\mathcal{H}^k(\boldsymbol{X}, \boldsymbol{N}) = \emptyset$ **then**
    break;
  end if
  Find the optimal solution t^* for problem (35) with $\boldsymbol{Y}^k$, $\boldsymbol{X}^k$, $\boldsymbol{N}^k$, $\mathcal{H}^k(\boldsymbol{X}, \boldsymbol{N})$, $\boldsymbol{\lambda}^k$.
  Suppose $\mathcal{H}^{k+1}(\boldsymbol{X}, \boldsymbol{N}) := \{j | t_j^* > 0, j \in \mathcal{W}\}$.
  Solve problem (36) with $\boldsymbol{Y}^k$, $\boldsymbol{X}^k$, $\boldsymbol{N}^k$, $\mathcal{H}^{k+1}(\boldsymbol{X}, \boldsymbol{N})$. Obtain the optimal solution $\boldsymbol{\lambda}^*$, set $\boldsymbol{\lambda}^{k+1} = \boldsymbol{\lambda}^*$.
end for

Proof. According to Lemma 5.1, when $Q \leq \sqrt{\frac{1-\varepsilon}{\varepsilon}}$, Algorithm 1 terminates in the second iteration with a termination criterion $\mathcal{H}^2(\boldsymbol{X}, \boldsymbol{N}) = \emptyset$. This criterion implies that constraints (28)–(30) are redundant. Therefore, RP-SOCP is equivalent to RP-1, in which the redundant constraints are removed. □

Define Z^D, Z^B, and Z^I as the optimal minimal costs (32) of RP-SOCP, the Bonferroni approximation, and the individual chance constraint, respectively. The following theorem holds:

Theorem 4.9. *The relations among Z^B, Z^I and Z^D are as follows,*

1. *If $Q < \sqrt{\frac{1-\varepsilon}{\varepsilon}}$, then $Z^D < Z^I$.*
2. *If $Q = \sqrt{\frac{1-\varepsilon}{\varepsilon}}$, then $Z^D = Z^I$.*
3. *If $Q > \sqrt{\frac{1-\varepsilon}{\varepsilon}}$, then $Z^I < Z^D < Z^B$.*

Proof. The proofs fall into the following three cases:

1. If $Q < \sqrt{\frac{1-\varepsilon}{\varepsilon}}$, $\mathcal{J} = \emptyset$ based on Proposition 4.7, then, $\boldsymbol{X}_j^T \boldsymbol{u} - N_j + Q\sqrt{\boldsymbol{X}_j^T \Gamma \boldsymbol{X}_j} < \boldsymbol{X}_j^T \boldsymbol{u} - N_j + \sqrt{\frac{1-\varepsilon}{\varepsilon}}\sqrt{\boldsymbol{X}_j^T \Gamma \boldsymbol{X}_j} \leq 0, \forall j \in \mathcal{W}$, which implies RP-SOCP is a relaxation of the program with individual chance constraints (20), thus, $Z^D < Z^I$.
2. If $Q = \sqrt{\frac{1-\varepsilon}{\varepsilon}}$, the proof is similar to that in case (1).
3. If $Q > \sqrt{\frac{1-\varepsilon}{\varepsilon}}$, when $j \in \mathcal{J}$, inequalities (28)–(30) are tighter than (21) as a result of Theorem 4.6; when $j \in \mathcal{W} \setminus \mathcal{J}$, $\boldsymbol{X}_j^T \boldsymbol{u} - N_j + Q\sqrt{\boldsymbol{X}_j^T \Gamma \boldsymbol{X}_j} \leq 0$ is sufficient for (21). Feasible domain of RP-SOCP dominates that of the program with individual chance constraints, that is, $Z^D > Z^I$. Based on Theorem 3.2 in Chen et al. (2010), $Z^D < Z^B$.

□

5. Solution approach

Although problem RP-SOCP can be solved by the procedure proposed by Chen et al. (2010), the solution process is time-consuming in general. However, a special case of the problem can be efficiently solved with an OA algorithm, as proposed here.

5.1. Solution procedure based on Chen et al. (2010)

The difficulty in Proposition 4.5 is to find the appropriate $\boldsymbol{\lambda}$ and $\mathcal{J}$ because $\Upsilon(\boldsymbol{N}, \boldsymbol{X}, \boldsymbol{\lambda}, \mathcal{J})$ is not jointly convex in $\boldsymbol{Y}$, $\boldsymbol{N}$ and $\boldsymbol{\lambda}$. However, if the value of $\boldsymbol{Y}$ and $\boldsymbol{N}$ are fixed, the value of $\boldsymbol{\lambda}$ can be iteratively improved by a SOCP, and we can always find a $\boldsymbol{\lambda} > 0$ and a set $\mathcal{J} \subseteq \mathcal{W}$ such that the RP-SOCP model is feasible (Chen et al., 2010). In order to improve upon the objective by readjusting the value of λ_j and the set $\mathcal{J}$, we need to get greater slack in model RP-SOCP. Defining $\mathcal{H}(\boldsymbol{X}, \boldsymbol{N}) = \left\{ j : \max_{j \in \mathcal{W}} \left[\mathbf{X}_j^T \boldsymbol{d} - N_j \right] > 0 \right\}$, the objective function (32) is improved iteratively by minimizing the total cost over λ_j, $j \in \mathcal{H}(\boldsymbol{X}, \boldsymbol{N})$. For a feasible solution ($\boldsymbol{X}, \boldsymbol{N}$) in RP-SOCP, we readjust $\mathcal{H}(\boldsymbol{X}, \boldsymbol{N})$ by solving problem (35):

$$\begin{array}{ll} \min\limits_{t} & \sum_{j=1}^{J} t_j, \\ s.t. & \boldsymbol{X}_j^T \boldsymbol{u} - N_j + Q\sqrt{\boldsymbol{X}_j^T \Gamma \boldsymbol{X}_j} \le t_j, \forall j \in \mathcal{W}, \\ & t \in \mathbb{R}. \end{array} \tag{35}$$

and update $\mathcal{H}(\boldsymbol{X}, \boldsymbol{N}) = \{j : t_j^* > 0\}$.

If set $\mathcal{H}(\boldsymbol{X}, \boldsymbol{N})$ is nonempty, the optimal $\boldsymbol{\lambda}^*$ can be obtained by solving problem (36).

$$\begin{array}{ll} \min\limits_{\lambda} & \Upsilon(\boldsymbol{N}, \boldsymbol{X}, \boldsymbol{\lambda}, \mathcal{H}), \\ s.t. & \sum_{j \in \mathcal{H}(\boldsymbol{X}, \boldsymbol{N})} \lambda_j = 1, \\ & \lambda_j \ge 0, \qquad \forall j \in \mathcal{H}(\boldsymbol{X}, \boldsymbol{N}). \end{array} \tag{36}$$

The corresponding procedure for improving the choice of $\boldsymbol{\lambda}$ and $\mathcal{H}(\boldsymbol{X}, \boldsymbol{N})$ is illustrated in Algorithm 1.

Generally, although Algorithm 1 is computationally excruciating, it terminates in the second iteration if $Q \le \sqrt{\frac{1-\varepsilon}{\varepsilon}}$, which is proved in Lemma 5.1.

Lemma 5.1. *When $Q \le \sqrt{\frac{1-\epsilon}{\epsilon}}$, Algorithm 1 terminates in the second iteration, with a termination criteria $\mathcal{H}^2(\boldsymbol{X}, \boldsymbol{N}) = \emptyset$.*

Proof. Because of the inequalities $\mathcal{H}^1(\boldsymbol{X}, \boldsymbol{N}) = \mathcal{W}$ in the first iteration of Algorithm 1, (28)–(30) dominate inequality (21) $\forall j \in \mathcal{W}$ according to Theorem 4.6. When $Q \le \sqrt{\frac{1-\varepsilon}{\varepsilon}}$,

$$\boldsymbol{X}_j^T \boldsymbol{u} - N_j + Q\sqrt{\boldsymbol{X}_j^T \Gamma \boldsymbol{X}_j} \le \boldsymbol{X}_j^T \boldsymbol{u} - N_j + \sqrt{\frac{1-\varepsilon}{\varepsilon}}\sqrt{\boldsymbol{X}_j^T \Gamma \boldsymbol{X}_j} \le 0,$$

and therefore, (21) is tighter than (33). Then, (33) holds under the condition that (28) –(30) are satisfied. Because problem (35) calculates the slack value of (33), then $t_j \le 0, \forall j \in \mathcal{W}$. That is, $\mathcal{H}^2(\boldsymbol{X}, \boldsymbol{N}) = \emptyset$, which terminates the algorithm in the second iteration. □

5.2. A customized outer approximation algorithm for solving RP-1

An OA algorithm is a cutting plane algorithm proposed by Duran and Grossmann (1987) to solve mixed-integer nonlinear programs (MINLPs). It iteratively decomposes an original MINLP into a nonlinear subproblem (SP) and a mixed-integer linear master problem (MP). The values of integer variables are fixed in SP, which provides an upper bound on the original MINLP. MP is implemented by a series of valid cuts based on the values of nonlinear terms and provides a lower bound. Fletcher and Leyffer (1994) and Bonami et al. (2008) state that an OA algorithm is an exact algorithm for MINLPs with convex continuous relaxations. Thus, we first prove the convexity of the continuous relaxation of RP-1 in Lemma 5.2.

Lemma 5.2. *RP-1 with continuously relaxed **Y** and **N** is convex.*

Proof. RP-1 is a linear program except for the nonlinear constraints (16) and (33); thus, it is sufficient to prove the convexity of (16) and (33). We define

$$\Phi(\boldsymbol{q}, r) = \sqrt{\boldsymbol{q}^T \boldsymbol{\Sigma} \boldsymbol{q}} - r, \tag{37}$$

$$\Psi(\boldsymbol{X}_j, \boldsymbol{N}_j) = Q\sqrt{\boldsymbol{X}_j^T \boldsymbol{\Sigma} \boldsymbol{X}_j} + \boldsymbol{X}_j^T \boldsymbol{u} - N_j. \tag{38}$$

Similar to Proposition 2 of Shahabi et al. (2014), $\Phi(\boldsymbol{q}, r)$ and $\Psi(\boldsymbol{X}, \boldsymbol{N})$ are convex. This completes the proof. □

5.2.1. Initialization

We myopically find a feasible solution to initiate the OA algorithm. First, only one facility is set up with the lowest unit construction cost, i.e., $Y_{j^*}^0 = 1,\ j^* = \{j | f_j = \min_{s \in J} f_s\}$. Then, for the demand sites that cannot be covered by the constructed facility, a separate facility is built, i.e., $Y_{j^\circ}^0 = 1,\ j^\circ = \{j | I \setminus I_{j^*}\}$. Finally, according to (8) and (9), $X_{ij}^0 = 1$ if $j = j^*$ and $j = j^\circ, \forall i \in I$; based on (33), the value of N_j^0 is $N_j = \left\lceil \boldsymbol{X}_j^{0^T} \boldsymbol{u} + Q\sqrt{\boldsymbol{X}_j^{0^T} \boldsymbol{\Gamma} \boldsymbol{X}_j^0} \right\rceil$.

5.2.2. OA subproblem

The subproblem finds the optimal values of continuous variables with fixed values of the integer variables. In iteration h, the input values of the integer variables are $\tilde{Y}_j^h$ and $\tilde{N}_j^h$, and SP can be summarized as follows:

$$\mathrm{SP} : \min\ \beta(\epsilon r + \boldsymbol{\mu}^T \boldsymbol{q}) + \sum_{j \in J} \left\{ f_j \tilde{Y}_j^h + a_j \tilde{N}_j^h \right\},$$

$$\begin{aligned} s.t.\ & \boldsymbol{X}_j^T \boldsymbol{u} - \tilde{N}_j^h + Q\sqrt{\boldsymbol{X}_j^T \boldsymbol{\Gamma} \boldsymbol{X}_j} \le 0, \forall j \in \mathcal{W}, \\ & X_{ij} \le \tilde{Y}_j^h, \forall i \in I, \forall j \in J, \\ & (8), (11), (15), (16), (17). \end{aligned}$$

5.2.3. OA master problem

The OA master problem is a mixed-integer linear program (MILP) and obtains the optimal solutions for continuous decision variables by utilizing the values of $\tilde{r}^h$, $\tilde{\boldsymbol{q}}^h$, and $\tilde{\boldsymbol{X}}^h$. The linear relaxations of nonlinear constraints (16) and (33) (OA cuts) are proved in Proposition 5.3.

Proposition 5.3. *The OA cuts associated with nonlinear constraints (16) and (33) in the hth iteration are as follows:*

$$\boldsymbol{q}^T \boldsymbol{\Sigma} \tilde{\boldsymbol{q}}^h - r\tilde{r}^h \le 0, \tag{39}$$

$$\left(\boldsymbol{X}_j^T \boldsymbol{u} - N_j\right)\sqrt{\tilde{\boldsymbol{X}}_j^{h^T} \boldsymbol{\Gamma} \tilde{\boldsymbol{X}}^h{}_j} + Q\boldsymbol{X}_j^T \boldsymbol{\Gamma} \tilde{\boldsymbol{X}}_j^h \le 0. \tag{40}$$

Proof. Considering the convexity of $\Phi(\boldsymbol{q}, \boldsymbol{r})$ and $\Psi(\boldsymbol{X}_j, \boldsymbol{N}_j)$, as shown in Lemma 5.2, and taking their first-order Taylor expansions, we obtain $\Phi(\tilde{\boldsymbol{q}}^h, \tilde{\boldsymbol{r}}^h) + \nabla\Phi(\tilde{\boldsymbol{q}}, \tilde{\boldsymbol{r}})\left[\boldsymbol{q} - \tilde{\boldsymbol{q}}^h, r - \tilde{r}^h\right]^T \le \Phi(\boldsymbol{q}, \boldsymbol{r}) \le 0$ and $\Psi(\tilde{\boldsymbol{X}}_j^h, \tilde{N}_j^h) + \nabla\Psi(\tilde{\boldsymbol{X}}_j^h, \tilde{\boldsymbol{N}}_j^h)\left[\boldsymbol{X}_j - \tilde{\boldsymbol{X}}_j^h, N_j - \tilde{N}_j^h\right]^T \le \Psi(\boldsymbol{X}_j, N_j) \le 0$, where $\nabla\Phi(\tilde{\boldsymbol{X}}_j^h, \tilde{\boldsymbol{N}}_j^h) = \left[\frac{(\tilde{\boldsymbol{q}}^h)^T \boldsymbol{\Gamma}}{\sqrt{(\tilde{\boldsymbol{q}}^h)^T \boldsymbol{\Gamma} \tilde{\boldsymbol{q}}^h}}, -1\right]$ and $\nabla\Psi(\tilde{\boldsymbol{X}}_j^h, \tilde{\boldsymbol{N}}_j^h) = \left[\boldsymbol{\mu}^T + \frac{Q(\tilde{\boldsymbol{X}}_j^h)^T \boldsymbol{\Gamma}}{\sqrt{\tilde{\boldsymbol{X}}_j^{h^T} \boldsymbol{\Gamma} \tilde{\boldsymbol{X}}_j^h}}, -1\right]$. Through simple algebra, we can obtain the closed-form solutions of OA cuts (39) and (40) because $\tilde{r}^h = (\tilde{\boldsymbol{q}})^T \boldsymbol{\Gamma} \tilde{\boldsymbol{q}}^h$. □

The OA master problem is summarized as follows:

$$\begin{aligned} \text{MP} : & \min \eta \\ & s.t.\ \eta \ge \beta(\epsilon r + \boldsymbol{\mu}^T \boldsymbol{q}) + \sum_{j \in J} \left\{ f_j Y_j + a_j N_j \right\}, \end{aligned} \tag{41}$$

$$\eta \le UB^h - \varepsilon, \forall h, \tag{42}$$

$$(8), (9), (11), (15), (16), (17), (39), (40).$$

where (41) defines the objective function and (42) ensures that the optimal solution to MP does not exceed the upper bound in the hth iteration (UB^h). We employ the ε-optimal OA framework proposed by Fletcher and Leyffer (1994) and terminate the algorithm whenever MP is infeasible. The OA procedure is illustrated in Algorithm 2.

Algorithm 2 OA algorithm.

Input: $\tilde{Y}_j^0$ and $\tilde{N}_j^0$: initial value of binary/integer decision variable Y_j and N_j.
LB^0: lower bound, equals to $-\infty$.
UB^0: upper bound, equals to ∞.
$\mathbb{K}$: the maximal number of iterations.

Procedure:
1: **for** $h = 1 : \mathbb{K}$ **do**
2: Solve SP. Get the optimal values of $\tilde{X}_{ij}^h$, $\tilde{q}_i^h$ and $\tilde{r}^h$, denote the optimal value of the objective function as upper bound UB^h.
3: Construct OA cuts (39) and (40) with fixed continuous variables $\tilde{X}_{ij}^h$, $\tilde{q}_i^h$ and $\tilde{r}^h$ and solve MP, obtain $\tilde{Y}_j^h$ and $\tilde{N}_j^h$, denote the optimal objective value as LB^h.
4: **if** MP is infeasible **then**
5: stop and return the incumbent value;
6: **end if**
7: **end for**

6. Numerical results

We conduct numerical experiments to test the efficiency and reliability of four methods of addressing the EMS location problem, including Bonferroni approximation, individual chance constraints, the scenario-based approach (see Appendix C),

Table 1
Comparison of the objective values between ScB, DRM, Bon and Ind.

$\|I\| = \|J\|$	ScB					DRM					Bon	Ind
	10	19	30	40	50	10	19	30	40	50		
10	0.97	0.97	0.99	0.99	1.00	0.98	1.00	1.01	1.02	1.03	1.13	1.00
15	0.92	0.93	0.94	0.94	0.96	0.96	1.00	1.12	1.15	1.18	1.38	1.00
20	0.98	0.99	0.99	1.00	1.00	0.98	1.00	1.02	1.04	1.05	1.28	1.00
25	0.83	0.84	0.84	0.85	0.85	0.96	1.00	1.03	1.06	1.08	1.51	1.00
30	0.82	0.82	0.83	0.83	0.84	0.97	1.00	1.03	1.05	1.08	1.48	1.00

and the DRM proposed in Section 6.1. Moreover, the performance of the proposed OA algorithm is also evaluated. We remark that individual chance constraints ensure local reliability for each demand site independently, while the other methods guarantee system reliability throughout the entire geographic area. The different network topologies determined by the solutions are compared in Section 6.3. Validations of the DRM are presented in Section 6.4. In addition, experiments with real-life data are reported in Section 6.5.

The numerical experiments are conducted on a computer with an Intel Core i9 Duo 3.40 GHz processor and 32GB of RAM. The Mosek Version 8.0.0.79 optimization toolbox for MATLAB (ApS, 2015) is employed to solve RP-SOCP, RP-1, and MP and SP of the OA algorithm. The solver terminates with a relative optimality tolerance equal to 0.01. YALMIP (Löfberg, 2004) is also used to enable the use of MATLAB.

6.1. Performance analysis

Twenty-five groups of tests with five instances for each are conducted. The number of facilities and demand sites, I and J, are equal with values of 10, 15, 20, 25 and 30. Q is the radius of the distributional set consisting of a random MNCD ($\boldsymbol{D}$). Q^2 is assigned as 10, 19, 30, 40 and 50. Twenty scenarios for $\boldsymbol{\Theta}$ and $\boldsymbol{D}$ each are generated in the scenario-based approach.

Experiments are generated on a 10×10 square, representing the demand sites and candidate facilities. Parameters are similar with those in Zhang and Li (2015) and are summarized as follows.

f_j	Uniformly generated from [25,75]
a_j	Uniformly generated from [1,3]
β	Equal to 5
α	Equal to 0.95
Θ_i	Uniformly generated from the distributional set defined in Eq. (12), $\boldsymbol{\Sigma}$ is positive semidefinite matrix, and $\boldsymbol{\mu}$ ∈U[0.1,5], $\sigma_i \sim U[0.5, 1.5]$; (daily) demand correlation coefficients $\rho_{ij}^{\Theta} = 0.1, \forall i \neq j \; \& \rho_{ij}^{\Theta} = 1, \forall i = j$
D_i	Uniformly generated from the distributional set defined in equation (18), $\boldsymbol{\Gamma}$ is a positive semidefinite matrix and $\boldsymbol{u}$ ∈U[0.1,10], $\gamma_i \sim U[0, 2]$; MNCD correlation coefficients $\rho_{ij}^{D} = 0.1, \forall i \neq j \; \& \rho_{ij}^{D} = 1, \forall i = j$

We use the data-driven method proposed by Delage and Ye (2010) and Zhang et al. (2016) to construct the distributional set $\mathcal{F}$ defined in (12). One thousand scenarios of randomly generated data for (daily) demand at each demand sites are obtained based on a multivariate normal distribution. The procedure for the data-driven approach is as follows: First, the sample mean and variance for $\boldsymbol{\Theta}$ are calculated as $\hat{\boldsymbol{\mu}}$ and $\boldsymbol{\Sigma}_0$. Then, based on (12), we suppose $\delta = 0.05$, $R^2 = \max_{m=1,\cdots,M} (\boldsymbol{\Theta}_m - \hat{\boldsymbol{\mu}})^T \boldsymbol{\Sigma}_0^{-1} (\boldsymbol{\Theta}_m - \hat{\boldsymbol{\mu}})$ and $\epsilon = (R/\sqrt{M})[2 + \sqrt{2\ln(1/\delta)}]$ to estimate the distributional sets for $\mathbb{E}(\boldsymbol{\Theta})$. distributional set $\mathcal{G}$ is an ellipsoid of radius Q ($Q = \sqrt{10}, \sqrt{19}, \sqrt{30}, \sqrt{40}, \sqrt{50}$). Finally, Algorithm 1 is applied with $\tau = 0.01$ and $K = 30$.

We compare the expected minimized total cost (objective value) of the conducted five instance determined by the solutions of scenario-based approach (ScB), the proposed DRM (DRM), Bonferroni approximation (Bon), and individual chance constraints (Ind) in Table 1. Note that Ind represents the program where the original individual chance constraints (20) are replaced with CVaR-based approximations (21). To highlight the comparison, the final results are translated into the ratio form; that is, the objective value of other algorithms/the objective value of individual chance constraints.

It is significant that when the radius Q of distributional set (18) decreases, which implies the uncertainty set of $\boldsymbol{D}$ becomes smaller, the benefit of exact estimation of uncertain MNCD is illustrated by less total cost. Based on Theorem 4.9, when $\varepsilon = 0.05$, $Q^2 = (1-\varepsilon)/\varepsilon = 19$, then $Z^I = Z^D$, the ratio of the objective value between the DRM when $Q^2 = 19$ and individual chance constraints are all equal to 1; similar results when $Q^2 < (1-\varepsilon)/\varepsilon$ and $Q^2 > (1-\varepsilon)/\varepsilon$ also verify the theorem. The theoretical and numerical results also reveal that the proposed DRM can effectively avoid the over-conservative results obtaining from the Bonferroni approximation. Because ScB randomly considers limited number of scenarios while DRM considers all possible scenarios, thus, the objective value of ScB is smaller than or equal to that of DRM. Compared with the individual chance constraints and the scenario-based approach, DRM yields a larger cost because of robustness; moreover, Section 6.4 shows a higher system reliability than the approaches mentioned above.

Table 2 reports the CPU running time results associated with ScB, DRM, Bon and Ind. The Bonferroni approximation can obtain the optimal solution within the shortest time and DRM comes in last. However, computational efficiency is not the most pivotal issue in a facility location problem compared with those in a real-time system. Moreover, there is no significant difference in the computational time for DRM with respect to Q when $|I|$ and $|J|$ are small; when $|I|$ and $|J|$ become larger

Table 2
A summary of CPU running time (specified in seconds) .

$\|I\| = \|J\|$	Bon	ScB				
		$Q^2 = 10$	$Q^2 = 19$	$Q^2 = 30$	$Q^2 = 40$	$Q^2 = 50$
10	1.10	3.22	3.51	3.44	3.57	5.04
	(0.36)	(0.39)	(0.41)	(0.45)	(0.72)	(0.88)
15	6.38	17.80	20.94	19.80	20.49	22.06
	(4.41)	(4.95)	(8.15)	(7.19)	(4.37)	(8.14)
20	59.29	78.57	73.80	85.30	72.65	79.70
	(19.30)	(23.98)	(22.69)	(31.74)	(18.53)	(29.76)
25	141.01	280.97	285.95	305.04	265.17	314.62
	(108.64)	(120.23)	(75.98)	(134.40)	(98.60)	(114.05)
30	1070.99	705.25	656.45	588.97	669.97	727.36
	(521.81)	(160.50)	(81.58)	(122.75)	(113.47)	(138.55)
$\|I\| = \|J\|$	Ind	DRM				
		$Q^2 = 10$	$Q^2 = 19$	$Q^2 = 30$	$Q^2 = 40$	$Q^2 = 50$
10	1.23	15.64	15.56	17.56	14.90	14.89
	(0.37)	(7.84)	(13.57)	(17.72)	(12.59)	(12.70)
15	11.19	79.09	75.01	87.98	87.73	84.68
	(6.56)	(36.19)	(31.51)	(25.36)	(25.37)	(25.90)
20	121.72	285.20	278.42	262.60	253.34	248.22
	(39.43)	(24.48)	(35.80)	(27.63)	(28.01)	(26.95)
25	502.89	1580.35	1430.90	1369.63	1352.11	1466.92
	(258.29)	(341.25)	(226.73)	(199.38)	(204.21)	(370.54)
30	7553.39	12403.49	11594.63	10967.14	9826.28	9166.01
	(4829.04)	(4819.81)	(5143.79)	(3562.55)	(3046.06)	(3009.20)

Table 3
Comparison between Mosek and OA in CPU running time (specified in seconds).

$\|I\| = \|J\|$	$Q^2 = 10$			$Q^2 = 19$		
	DRM	Mosek	OA	DRM	Mosek	OA
10	15.64	0.31	0.14	15.56	0.29	0.14
15	79.09	1.07	0.30	75.01	1.14	0.32
20	285.2	6.33	1.39	278.42	2.28	0.76
25	1580.35	40.25	6.12	1430.90	37.11	5.69
30	12403.49	1216.15	17.92	11594.63	197.52	6.62
35	14400.00*	7296.62	74.80	14400.00*	7358.82	69.84
40	14400.00*	14400.00*	396.03	14400.00*	14400.00*	401.43
45	14400.00*	14400.00*	742.57	14400.00*	14400.00*	1075.07
50	14400.00*	14400.00*	4874.18	14400.00*	14400.00*	4835.95

and $Q^2 \geq 19$, running time tends to become shorter. CPU running time with respect to the scenario-based approach doesn't show a monotonous trend.

Five instances for nine levels of $|I|$ and $|J|$ are randomly generated to illustrate the computational efficiency of the special case ($Q^2 = 10$ and $Q^2 = 19$). Table 3 reports the expected CPU running time of five instances associated with the three solution approaches. The "DRM" column shows the results of solving RP-SOCP with Algorithm 1. "Mosek" represents the results of directly solving RP-1 with Mosek, and the "OA" column reports the CPU running time for solving RP-1 with the proposed OA algorithm. The time limit for the solution approaches is set to 14,400 s. Results with a superscript * indicate that the optimal solutions for all instances cannot be found within the time limit, while in the other cases, the optimal solutions are obtained.

The results illustrate that the OA algorithm significantly outperforms the other two solution approaches. The comparison between "Mosek" and "DRM" confirms that the properties obtained by Lemmas 5.1 and 4.8 can help to speed up the solution process for the original EMS location and sizing problem when the uncertainty set is relatively small.

6.2. Sensitivity analysis

Sensitivity analysis of unit transportation cost (β) and expectation of MNCD ($\boldsymbol{u}$) are considered, experiments are conducted with the same input parameters except for the one for sensitivity analysis. Figures in each subsection illustrate the total cost (blue dashed line), total number of constructed facilities (values of the bars) and total number of ambulances (values in the brackets).

6.2.1. Sensitivity analysis of unit transportation cost (β)

As shown in Fig. 1, the total cost of an EMS system proportionally increases when β becomes larger. The total number of ambulances and number of constructed facilities also increase with β. This dynamic is because the growth of the total

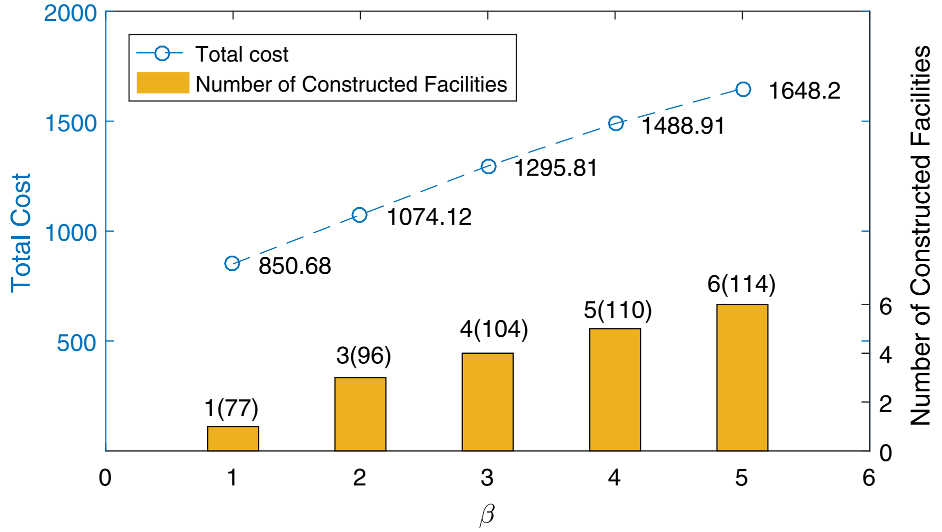

Fig. 1. Sensitivity analysis of Transportation Cost (β).

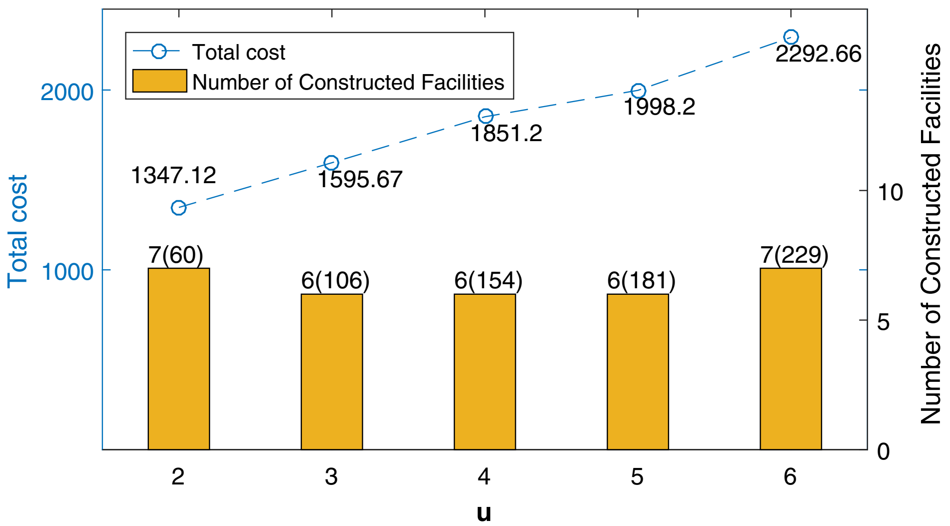

Fig. 2. Sensitivity analysis of mean MNCD ($\boldsymbol{u}$).

number of ambulances and the number of open facilities can effectively decrease the travel distance during a relief response, which in turn avoids increasing the transportation cost due to the large β.

6.2.2. *Sensitivity analysis of the expected MNCD at each site* (u)

We consider the effect of the expected MNCD ($\boldsymbol{u}$) at each demand site. Fig. 2 illustrates that the total cost and total number of ambulances both grow proportionally as the expected MNCD increases. On the other hand, the number of constructed facilities remains almost unchanged, which suggests that the variation of $\boldsymbol{u}$ does not have a significant influence on facility location decisions. The growing MNCD is satisfied by increasing the number of ambulances.

6.3. *Topology analysis*

We compare topology networks determined by the solutions of methodologies that ensure the reliability level on the entire geographical area, i.e., Bon, Scb and DRM. To do so, we randomly generate 10 random graphs with 25 nodes for each on a 10 × 10 square, representing the demand points and potential facility locations. Other parameters are the same as described in Section 6.1. A typical solution is summarized in Fig. 3. In the figures, black dots denote the locations of facility candidates (co-located with the demand sites); red circles indicate that the associated facility is open, and the thickness of

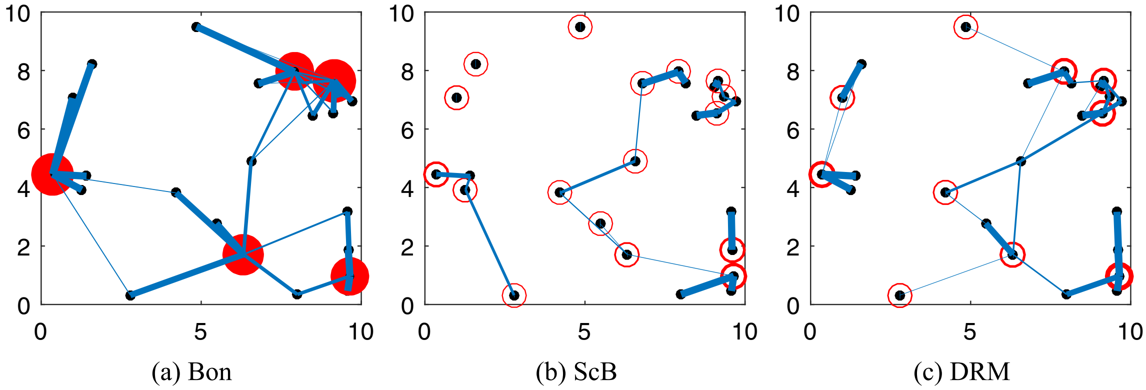

Fig. 3. Topology analysis of Bon, ScB and DRM.

Table 4
The definitions of M#EF, M#DF, M#CF and MTD.

Properties for facilities	M#EF	M#DF
Definition	$\sum_j \sum_i \mathcal{I}\{X_{ij} > 0\} / \sum_j Y_j$	$\Sigma_j \Sigma_i [d_i X_{ij}] / \Sigma_j Y_j$
Properties for demand sites	M#CF	MTD
Definition	$\sum_i \sum_j \mathcal{I}\{X_{ij} > 0\} / I$	$\Sigma_i \Sigma_j [c_{ij} X_{ij}] / I$

Table 5
Comparing the topology of the three methodologies.

	Total cost	TY	TN	M#EF	M#DF	M#CF	MTD
Bon	4065.090	5	461	8.000	10.800	1.600	1.474
ScB	2208.111	17	194	2.059	3.176	1.400	0.469
DRM	2292.330	10	219	3.800	5.400	1.520	0.699

red circles represents the number of ambulances held by that facility; blue lines illustrate the demand coverage, and the thickness is proportional to the percentage of allocation.

We define mean number of edges/facility (M#EF), mean number of demand/facility (M#DF) as properties for facilities (Baron et al., 2011); mean number of connected facilities per demand sites (M#CF), mean travel distance (MTD) as properties for demand sites in Table 4, where $\mathcal{I}(\cdot)$ is the indicator function.

Total cost (TC), total number of constructed facilities (TY), total number of ambulances (TN), M#EF M#DF, M#CF and MTD are reported in Table 5. We make several observations.

1. In terms of different total number of constructed facilities and ambulances, the topology network obtained by the scenario-based approach tends to open more facilities with fewer ambulances. In contrast, Bonferroni approximation establishes fewer facilities with a larger number of ambulances. The topology network obtained by the DRM is a compromise of the scenario-based approach and the Bonferroni approximation. DRM constructs a modest number of facilities, and an appropriate number of ambulances are assigned, combining the advantages of the other methodologies.
2. In terms of the properties for constructed facilities, mean number of connected demand sites and the mean number of arranged demand load under the Bonferroni approximation are 8.0 and 10.8 respectively, which are significantly larger than those in the scenario-based approach and the proposed DRM. However, centralized network topology like the Bonferroni approximation may face higher disruption risk in disasters, as the breakdown of any open facility may cause demand shortage in a large number of demand sites.
3. In terms of the properties for demand sites, mean number of connected facilities are similar in Bon, ScB and DRM. Demands at each demand sites are satisfied by more than one open facilities in all the three methodologies, which expresses flexibility and robustness facing demand uncertainty. As for weighted travel distance, we find the transportation cost for the scenario-based approach and the proposed DRM take 31.85% and 47.46% of that in the Bonferroni approximation.

6.4. Validation

In this section, a Monte Carlo simulation is employed to valid the proposed DRM. We assume $\rho_{ij}^D = 0, \forall i \neq j$, other parameters are the same with those in Section 6.1, and simulate the probability of satisfying demand in the entire geographic

Table 6
Monte Carlo simulation between Bon, Ind, ScB, DRM.

Open	$\alpha = 0.60$				$\alpha = 0.70$				$\alpha = 0.80$			
facility	Bon	Ind	ScB	DRM	Bon	Ind	ScB	DRM	Bon	Ind	ScB	DRM
2	1.00	0.89	1.00	1.00	1.00	0.94	1.00	1.00	1.00	0.98	1.00	1.00
5	-	-	1.00	-	-	0.94	1.00	-	-	-	-	-
6	1.00	0.89	1.00	1.00	1.00	0.98	1.00	1.00	1.00	0.98	1.00	1.00
7	-	0.89	1.00	-	-	0.98	1.00	-	-	0.98	-	-
8	1.00	0.90	1.00	1.00	1.00	0.96	1.00	1.00	1.00	0.98	1.00	1.00
9	1.00	0.97	1.00	1.00	1.00	0.95	1.00	1.00	1.00	0.98	1.00	1.00
12	1.00	0.98	1.00	1.00	1.00	0.97	1.00	1.00	1.00	0.98	1.00	1.00
14	1.00	0.97	1.00	1.00	1.00	0.98	1.00	1.00	1.00	0.98	1.00	1.00
15	-	0.89	-	-	-	-	-	-	-	-	-	-
16	1.00	0.92	1.00	1.00	1.00	0.94	1.00	1.00	1.00	0.98	1.00	1.00
17	1.00	0.89	1.00	1.00	1.00	0.94	1.00	1.00	1.00	0.98	1.00	1.00
18	1.00	0.89	0.50	1.00	1.00	0.94	0.76	1.00	1.00	0.98	0.76	1.00
19	-	0.89	0.50	1.00	-	0.94	0.76	-	-	0.98	0.76	-
20	-	0.89	0.92	-	-	0.94	0.92	-	-	0.98	1.00	-
21	-	0.89	1.00	-	-	0.93	1.00	-	-	0.98	1.00	-
22	-	0.97	1.00	1.00	-	0.97	1.00	1.00	-	0.98	1.00	1.00
24	-	0.96	1.00	-	-	0.94	-	-	-	0.98	1.00	-
25	1.00	0.92	-	1.00	1.00	-	-	1.00	1.00	0.98	1.00	1.00
26	1.00	0.96	0.98	1.00	1.00	0.94	0.98	1.00	-	0.98	0.98	1.00
27	-	0.89	0.98	-	-	0.94	0.98	-	-	0.98	0.98	-
29	-	0.89	0.22	-	-	0.94	0.98	-	-	0.98	0.98	-
30	1.00	0.92	1.00	1.00	1.00	0.94	1.00	1.00	1.00	0.98	1.00	1.00
Reliability	1.00	0.16	**0.05**	1.00	1.00	0.34	**0.50**	1.00	1.00	0.66	**0.54**	1.00
Open	$\alpha = 0.90$				$\alpha = 0.95$				$\alpha = 0.99$			
facility	Bon	Ind	ScB	DRM	Bon	Ind	ScB	DRM	Bon	Ind	ScB	DRM
2	1.00	1.00	1.00	1.00	1.00	1.00	1.00	1.00	1.00	1.00	1.00	1.00
5	-	-	1.00	-	-	-	1.00	-	-	-	1.00	-
6	-	1.00	1.00	1.00	-	1.00	1.00	1.00	-	1.00	1.00	1.00
7	-	1.00	1.00	-	-	1.00	1.00	-	-	-	1.00	-
8	1.00	1.00	1.00	1.00	1.00	1.00	1.00	1.00	1.00	1.00	1.00	1.00
9	1.00	1.00	1.00	1.00	1.00	1.00	1.00	1.00	-	1.00	1.00	1.00
12	1.00	1.00	1.00	1.00	-	1.00	1.00	1.00	-	1.00	1.00	1.00
14	1.00	1.00	1.00	1.00	-	1.00	1.00	1.00	-	1.00	1.00	1.00
16	1.00	1.00	1.00	1.00	1.00	1.00	1.00	1.00	1.00	1.00	1.00	1.00
17	-	1.00	1.00	1.00	-	1.00	1.00	1.00	-	1.00	1.00	1.00
18	1.00	1.00	0.81	1.00	1.00	1.00	0.81	1.00	1.00	1.00	0.81	1.00
19	-	1.00	0.76	-	-	1.00	0.76	-	-	-	0.76	-
20	-	1.00	1.00	-	-	1.00	1.00	-	-	-	1.00	-
21	-	1.00	1.00	-	-	1.00	1.00	-	-	-	1.00	-
22	1.00	1.00	1.00	1.00	-	1.00	1.00	1.00	-	-	1.00	1.00
24	-	1.00	1.00	-	-	-	1.00	-	-	-	-	-
25	-	1.00	-	1.00	-	1.00	-	1.00	-	1.00	-	1.00
26	-	1.00	1.00	1.00	-	1.00	1.00	1.00	-	1.00	1.00	1.00
27	-	1.00	0.98	-	-	1.00	1.00	-	-	-	1.00	-
29	-	-	0.98	-	-	-	0.99	-	-	-	1.00	-
30	-	1.00	1.00	1.00	-	1.00	1.00	1.00	-	1.00	1.00	1.00
Reliability	1.00	0.98	**0.59**	1.00	1.00	1.00	**0.61**	1.00	1.00	1.00	**0.62**	1.00

areas obtained from the four solution methodologies, including Bon, Ind, ScB and DRM, when reliability level α changes from 0.6 to 0.99. The Monte Carlo simulation procedure is employed as follows.

Step 1: Supposing $I = J = 30$ and $Q^2 = 50$, obtain the optimal EMS networks and the corresponding ambulance numbers at each EMS station.
Step 2: Uniformly generate 100,000 samples of MNCD at each demand site within distributional set (16).
Step 3: Calculate the ratio of satisfied demand for all open facilities.

The ratios of satisfied demand in all samples are presented in Table 6. The first column lists the open EMS facilities. Symbol " - " in Table 6 indicates that the corresponding facility is not constructed. As shown in Table 6, all the approximated reliability levels exceed the predetermined α separately. Table 6 also summarizes the system reliabilities associated with the four approaches. We define

$$\text{Reliability} = \prod_{j \in \mathcal{P}} p_j,$$

where $\mathcal{P} = \{j | Y_j = 1\}$, p_j denotes the probability of satisfying demand at demand site j in the Monte Carlo simulation.

Table 7
Comparison of five approaches with real data.

	Bon	I-A	I-S	I-U	DRM
Ratio of total cost	1.234	0.966	0.950	0.935	1.000
Ratio of CPU time	0.212	0.619	0.754	0.868	1.000

Table 8
Monte Carlo simulation for real data.

	Open facility	Bon	I-A	I-S	I-U	DRM
Arbitrary random variables	8	1.0000	0.9860	1.0000	1.0000	1.0000
	9	1.0000	1.0000	0.9560	0.9690	1.0000
	24	1.0000	0.9900	0.9070	0.8820	1.0000
	Reliability	1.0000	0.9761	0.8671	0.8547	1.0000
Multivariate-normal-distributed random variables	8	1.0000	1.0000	1.0000	1.0000	1.0000
	9	1.0000	1.0000	0.9993	0.9997	1.0000
	24	1.0000	1.0000	0.9988	0.9977	1.0000
	Reliability	1.0000	1.0000	0.9981	0.9974	1.0000

Although individual chance constraints and the scenario-based approach obtain a reliability level higher than the predetermined level in each demand site independently, the system reliability is poor. In contrast, the results from the Bonferroni approximation and the proposed DRM are much more stable. Moreover, the proposed DRM can avoid the over-conservatism resulting from the Bonferroni approximation and reduce total cost, as shown in Table 1. Furthermore, when α becomes larger, the reliability may become smaller in the scenario-based approach since the selected samples are randomly generated. However, this dynamic has not been observed in the results associated with the other three methods based on robust optimization.

6.5. Experimentation with real-life data and value of the DRM

We apply the proposed DRM to the 30 datasets in Zhang and Li (2015). The cost-related parameters and the calculation of MNCD are the same as those in Zhang and Li (2015), and we suppose $\alpha = 0.95$. One thousand samples of historical data for daily demand and MNCD are obtained, the distributional set of $\mathbb{E}_F(\boldsymbol{\Theta})$ (12) is estimated in the same way of Section 6.1. The distributional set of MNCD ($\boldsymbol{D}$) (18) is obtained by $Q^2 = \max_{m=1,\cdots,M} (\boldsymbol{D}_m - \hat{\boldsymbol{u}})^T \boldsymbol{\Gamma}_0^{-1} (\boldsymbol{D}_m - \hat{\boldsymbol{u}})$, where $\hat{\boldsymbol{u}}$ and $\boldsymbol{\Gamma}_0$ are the sample mean and variance of $\boldsymbol{D}$.

In order to test algorithm performance in the application, we compare the proposed DRM with the approaches considered in Zhang and Li (2015), in which three different approximations for individual chance constraints are considered when the MNCD represents arbitrary, symmetric and unimodal symmetric random variables. The experiments for the Bonferroni approximation are also conducted for comparison. The results are reported in Tables 7 and 8. In the first row of the tables, “I-A”, “I-S”, “I-U” represent individual chance constraints for an arbitrary, symmetric, unimodal symmetric random variable, respectively. Note that“I-A” is the same with Ind and that“I-S” and “I-U” represent approximated individual chance constraints with more information on the distribution, and these terms are less conservative than “I-A”.

Table 7 summarizes the minimized total cost and the CPU running time, to highlight the comparison, the final results are translated into the ratio form; that is, other algorithms/DRM. Recall that individual chance constraints only guarantee the probability of satisfying demand in each demand sites independently, while Bon and DRM ensure system reliability in the entire geographic area. Total costs of Bon and DRM are larger than those of the approach proposed in Zhang and Li (2015) because of robustness. Compared with DRM, the Bonferroni approximation increases total cost by 23.4%, while the other three approximations for individual chance constraints drop total cost up by 7%.

Table 8 reports the Monte Carlo simulation results similar to the procedure described in Section 6.4. One hundred thousand samples of $\boldsymbol{\Theta}$ are generated within the distributional set (12) when $\epsilon = 8.493$ according to the data-driven approach described in Section 6.1. Two kinds of samples are generated to test the probability of satisfying MNCD in each demand sites and the entire geographic area: ① Arbitrary random variables uniformly generated within the distributional set (18). ② Multivariate-normal-distributed random variables with mean $\hat{\boldsymbol{u}}$ and covariance matrix $\boldsymbol{\Gamma}_0$.

As shown in Table 8, if MNCD are arbitrary random variables, the approximated service levels for each open facility in Bon, I-A, DRM are greater than 0.95. Since the random samples are not guaranteed to be symmetric or unimodal symmetric, the service levels in I-S and I-U are not necessarily larger than 0.95. In the case described in Table 8, only three facilities are opened, for I-A, I-S and I-U, the product of $p_j \geq 0.95, j = 8, 9, 24$ can be greater than 0.95, which implies to ensure the system reliability. However, this is only the case in numerical results, theoretically, Bon and DRM ensure system reliability while I-A, I-S and I-U ensure local reliability.

Nevertheless, regarding system reliability, the Bonferroni approximation and the proposed DRM are more efficient than the other three approaches. If MNCD are normally-distributed random variables, the probability of satisfying demands in each site is larger than 0.95 in all of the five approaches. To sum up, if no other distribution information of MNCD is available except for the first and second moments, DRM can obtain a solution with higher system reliability and lower cost in the real application.

7. Discussion of the extended application of the model in disaster management

An effective EMS system does not merely manage common emergencies (such as household fires, first-aid treatment and vehicle accidents) but also provides medical relief supplies in the wake of large-scale disasters (earthquake, tsunami, bioterrorism attack, explosion, etc.) with a very short response time. Research on disaster operations management and humanitarian logistics has grown rapidly in the past few years. Emergency management can generally be divided into three phases: preparedness, (post-disaster) response and recovery (Özdamar and Ertem, 2015). The storage location and inventory levels for medical supplies should be determined in the preparedness phase, thereby mitigating the risk of incurring a catastrophic disaster. Recent large-scale disasters have underscored the need for effective and efficient public health and medical responses (Brandeau et al., 2009). In 2005, Hurricanes Katrina, Wilma and Rita caused more than $ 100 billion in damage because of the inadequacy of prepositioning strategies. Since then, preparedness plans have been brought to the forefront of academic attention. Most studies formulated the prepositioning of relief materials (such as water, food or medical kits) by means of a two-stage stochastic programming problem (Ukkusuri and Yushimito, 2008; Rawls and Turnquist, 2010; Kınay et al., 2018), where some unique identities of disasters, such as booming demand (Jia et al., 2007) and uncertain network conditions (Özgün Elçi et al., 2018), are well-characterized.

The optimization techniques of regular emergencies and large-scale disasters can be similar in the preparedness phase. Location, inventory and distribution strategies are the main concerns in both cases. From the perspective of performance metrics, Gralla et al. (2014) and Yu et al. (2018) stated that efficiency, effectiveness and equity should be considered in the relief process of large-scale disasters, as reflected in the EMS system. Each of the three metrics corresponds to a concrete characteristic in the mathematical model. First, Gralla et al. (2014) determined efficiency by calculating the system-wide economic cost. A large variety of literature employs cost-related objectives (Rawls and Turnquist, 2010; Noyan, 2012; Chen and Yu, 2016; Ni et al., 2018), and our work does the same. Second, service quality is a measure of system effectiveness. Some studies minimized unsatisfied demand (Özdamar et al., 2004) or undistributed supplies (Orgut et al., 2016) in the objective function; others used chance constraints to ensure a satisfactory service level (Hong et al., 2014; Liu et al., 2016). Our research falls into the latter category. Third, equity means the fairness of victims from different areas. Since the main aim of disaster management is to provide early response, equity is expressed as a function of distance or response time in previous research. Kınay et al. (2018) matched the nearest open shelter to vulnerable areas. Yang et al. (2013) studied a discrete resource allocation problem minimizing the range of waiting time in public services. Similar to Hong et al. (2014), we minimize the transportation costs, which is helpful to reducing response times. Note that cost efficiency is not a major concern for decision makers in the disaster case compared with regular emergencies. Effectiveness and equity are more important than cost efficiency. Different objectives, such as demand coverage (Chanta and Sangsawang, 2012), response time (Bayram et al., 2015) and accessibility (Özgün Elçi et al., 2018), can also be considered.

Two major distinct features of disasters are tremendous demand and low-frequency. The lack of historical data makes demand prediction and disaster prevention much more difficult than daily EMS cases. Thus, in the disaster case, the following approaches can be considered to construct reliable estimates of random demand. First, we can predict maximum concurrent demand based on the unique attributes of different demand sites, such as population density, economic importance, geographical features and weather patterns (Jia et al., 2007). Second, simulation systems can be introduced to forecast and prepare data during disasters (Horner, 2008; Lee et al., 2009). Third, artificial intelligence can be applied to forecast short-term natural disasters (Hoyos et al., 2015). For example, backpropagation artificial neural networks were successfully applied to forecast typhoon (Lee, 2008) and heavy snow disasters (Wu et al., 2008). Finally, expert opinion can help to create reliable predicted disaster scenarios and demand data (Chang et al., 2007; Rawls and Turnquist, 2010).

After obtaining reliable estimates of the random variables and exogenous parameters, distributionally robust optimization is a perfect data-driven approach to make decisions in emergency management. In practice, the exact distributions of random variables are difficult to estimate with limited data; thus, researchers can take advantage of available data to estimate certain moments and distribution properties. DRO is an intermediate approach between stochastic optimization, which has no robustness to distribution error, and robust optimization, which ignores the available problem data (Delage and Ye, 2010).

In summary, on account of similar decision variables and performance metrics, our model can be extended to large-scale disasters only if the ambiguity sets and parameters can be adjusted based on the unique features. To make the model more practical and reliable, uncertain network conditions, other performance-related objectives and different types of shelters can be taken into consideration in the disaster case.

8. Conclusion

The principal purpose of this research is to support emergency relief planners in developing long-term EMS system designs, including facility locations and stock pre-positioning decisions that enable efficient medical relief responses for daily demand or large-scale emergencies. To handle the inherent uncertainty in EMS systems, we propose a two-stage stochastic programming model with joint chance constraints for the design of a reliable EMS network. Then, the model is approximated as a computationally tractable mixed integer conic quadratic program using a distributional robust optimization

(DRO) method. The benefits of the proposed DRO-based model are illustrated by comparing with three well-known approaches (the Bonferroni approximation, individual chance constraints and the scenario-based approach).

Based on the extensive numerical experiments, we find the following remarks: (1) In terms of the performance of different solution approaches, DRM achieves a higher reliability than the individual chance constraints, efficiently avoids the over-conservative results obtained by the Bonferroni approximation, and thoroughly considered all possible scenarios compared with the scenario-based approach; (2) When the distributional set of MNCD is small, which implies the estimation of random variable is accurate enough, individual chance constraints can ensure the system reliability because of its robustness, however, DRM can achieve the system reliability with a lower cost. (3) The topology network obtained by methodologies that ensure system reliability (Bon, Ind, Scb) tend to establish more than one facilities to service a single demand site, which illustrates the flexibility when facing demand uncertainty.

In future research, highly effective algorithms can be studied to tackle large-scale instances of the parametric SOCP. It would also be interesting to compare the results of other distributional sets in DRO. Moreover, an integration model considering other measurements, such as equity and response time, can be studied to generate more valuable management insights. Furthermore, better approximations on robust EMS location and sizing problems can be developed.

Acknowledgments

This research is partly supported by the National Natural Science Foundation of China (grant numbers 71771135), and the State Key Program of National Natural Science Foundation of China (grant number 71332005).

Appendix A. Proof of Theorem 4.1

Proof. From (7), it is obvious that

$$\mathbb{E}_F[g(\boldsymbol{Y},\boldsymbol{N},\boldsymbol{\theta})] = \beta(\boldsymbol{q}^*)^T\mathbb{E}_F[\boldsymbol{\Theta}] = \min_{\boldsymbol{X}\in\Omega(\boldsymbol{Y},\boldsymbol{N})} \boldsymbol{q}^T\mathbb{E}_F[\boldsymbol{\Theta}],$$

where $\Omega(\boldsymbol{Y}, \boldsymbol{N})$ is defined by constraints (8)–(11). We can obtain,

$$\sup_{F\in\mathcal{F}}\mathbb{E}_F[g(\boldsymbol{Y},\boldsymbol{N},\boldsymbol{\theta})] = \beta\sup_{F\in\mathcal{F}}\min_{\boldsymbol{X}\in\Omega(\boldsymbol{Y},\boldsymbol{N})} \boldsymbol{q}^T\mathbb{E}_F[\boldsymbol{\Theta}] = \beta\max_{F\in\mathcal{F}}\min_{\boldsymbol{X}\in\Omega(\boldsymbol{Y},\boldsymbol{N})} \boldsymbol{q}^T\mathbb{E}_F[\boldsymbol{\Theta}]. \tag{A.1}$$

The order of the max-min operation in (A.1) is equivalent to the corresponding min-max representation. For the optimal solution $\boldsymbol{q}^*$, we have

$$\max_{F\in\mathcal{F}}\min_{\boldsymbol{X}\in\Omega(\boldsymbol{Y},\boldsymbol{N})} \boldsymbol{q}^T\mathbb{E}_F[\boldsymbol{\Theta}] = \max_{F\in\mathcal{F}}(\boldsymbol{q}^*)^T\mathbb{E}_F[\boldsymbol{\Theta}] \geq \min_{\mathbb{E}[\boldsymbol{\Theta}]\in\Lambda}\max_{F\in\mathcal{F}}(\boldsymbol{q})^T\mathbb{E}_F[\boldsymbol{\Theta}],$$

where $\Lambda = \{x\in\mathbb{R}^T : (x-\mu)^T\Sigma^{-1}(x-\mu)\geq\epsilon^2\}\subseteq\mathbb{R}^T_+$.

In the second stage, there exists an optimal solution $(\boldsymbol{X}^*, \boldsymbol{q}^*)$ for $g(\boldsymbol{Y}, \boldsymbol{N}, \boldsymbol{\theta})$, then

$$\max_{\mathbb{E}[\boldsymbol{\Theta}]\in\Lambda}\min_{\boldsymbol{X}\in\Omega(\boldsymbol{Y},\boldsymbol{N})} \boldsymbol{q}^T\mathbb{E}_F[\boldsymbol{\Theta}] = \max_{\mathbb{E}[\boldsymbol{\Theta}]\in\Lambda}(\boldsymbol{q}^*)^T\mathbb{E}[\boldsymbol{\Theta}], \geq \min_{\boldsymbol{X}\in\Omega(\boldsymbol{Y},\boldsymbol{N})}\max_{\mathbb{E}[\boldsymbol{\Theta}]\in\Lambda} \boldsymbol{q}^T\mathbb{E}_F[\boldsymbol{\Theta}].$$

The first equality holds because $\boldsymbol{q}^*$ is the optimal solution for the second stage. Furthermore, since $\boldsymbol{X}^*\in\Omega(\boldsymbol{Y}, \boldsymbol{N})$, the second inequality is straightforward. The other direction holds from the minimax inequality (Fan, 1972). Based on the mean-covariance information of Θ, $\max_{\boldsymbol{x}\in\Lambda}\boldsymbol{q}^T\boldsymbol{x} = \epsilon\sqrt{\boldsymbol{q}^T\boldsymbol{\Sigma}\boldsymbol{q}} + \boldsymbol{\mu}^T\boldsymbol{q}$, problem P can be reformulated as

$$\begin{aligned}
&\min_{r,\boldsymbol{q},\boldsymbol{X},\boldsymbol{Y},\boldsymbol{N}} \epsilon\sqrt{\boldsymbol{q}^T\boldsymbol{\Sigma}\boldsymbol{q}} + \boldsymbol{\mu}^T\boldsymbol{q} + \sum_{j\in J}\{f_jY_j + a_jN_j\},\\
&s.t.\quad q_i = \sum\nolimits_{j\in J} c_{ij}X_{ij}, \forall i,\\
&\qquad\ \ q\geq 0, (4)\sim(6), (8)\sim(11).
\end{aligned}$$

Thus, Theorem 4.1 is proved by introducing a dummy variable r. □

Appendix B. Proof of Proposition 4.5

Proof. The robust counterpart (27) implies $\mathbb{P}\left(\mathbf{X}_j^T\mathbf{d} - N_j > 0\right) = 0, \forall j\in\mathcal{W}\setminus\mathcal{J}$. Thus, with $\boldsymbol{\lambda} > 0$ we have, $\mathbb{P}\left(\boldsymbol{X}_j^T\boldsymbol{d} - N_j \leq 0, \forall j\in\mathcal{W}\right) = \mathbb{P}\left\{\max_{j\in\mathcal{J}}\left(\lambda_j\left[\boldsymbol{X}_j^T\boldsymbol{d} - N_j\right]\right)\leq 0\right\}$. Based on Proposition 4.4, CVaR constraint (10) is the tightest convex approximation to individual chance constraints. Then, if $(\boldsymbol{N}, \boldsymbol{X})$ are feasible in chance constraint, it is sufficient to show that $\varrho_{1-\varepsilon}\left[\max_{j\in\mathcal{J}}\left[\lambda_j\left(\boldsymbol{X}_j^T\boldsymbol{d} - N_j\right)\right]\right]\leq 0$. Based on the classical inequality proposed by Meilijson and Nádas (1979),

$$\mathbb{E}\left(\max_{i=1,\cdots,n} A_i - \iota\right)^+ \leq \mathbb{E}(B-\iota)^+ + \sum_{i=1}^{n}\mathbb{E}(A_i - B)^+,\ \text{ for any r.v. B.}$$

Let $B = \boldsymbol{w}^T\boldsymbol{d} - w_0$, we obtain

$$
\begin{aligned}
& \varrho_{1-\varepsilon}\left[\max_{j\in\mathcal{J}}\left[\lambda_j\left(\boldsymbol{X}_j^T\boldsymbol{d} - N_j\right)\right]\right] \\
&= \min_{\iota}\left\{\iota + \frac{1}{\varepsilon}\mathbb{E}\left[\left(\max_{j\in\mathcal{J}}\left[\lambda_j\left(\boldsymbol{X}_j^T\boldsymbol{d} - N_j\right)\right] - \iota\right)^+\right]\right\} \\
&\le \min_{\iota,\boldsymbol{w},w_0}\left\{\iota + \frac{1}{\varepsilon}\left[\mathbb{E}[(\boldsymbol{w}^T\boldsymbol{d} - w_0 - \iota)^+] + \sum_{j\in\mathcal{J}}\mathbb{E}\left[\left([\lambda_j\boldsymbol{X}_j - \boldsymbol{w}]^T\boldsymbol{d} - \lambda_j N_j + w_0\right)^+\right]\right]\right\} \\
&\le \min_{\iota,\boldsymbol{w},w_0}\left\{\iota + \frac{1}{\varepsilon}\left[\pi\left(w_0 + \iota, \boldsymbol{w}\right) + \sum_{j\in\mathcal{J}}\pi\left(\lambda_j N_j - w_0, \lambda_j\boldsymbol{X}_j - \boldsymbol{w}\right)\right]\right\} \\
&= \min_{w_0,\boldsymbol{w}}\left\{\min_{\iota}\left[\iota + \frac{\pi\left(w_0 + \iota, \boldsymbol{w}\right)}{\varepsilon}\right] + \frac{1}{\varepsilon}\left[\sum_{j\in\mathcal{J}}\pi\left(\lambda_j N_j - w_0, \lambda_j\boldsymbol{X}_j - \boldsymbol{w}\right)\right]\right\} \\
&= \Upsilon\left(\boldsymbol{N}, \boldsymbol{X}, \boldsymbol{\lambda}, \mathcal{J}\right)
\end{aligned}
$$

Then, if $\Upsilon(\boldsymbol{N}, \boldsymbol{X}, \boldsymbol{\lambda}, \mathcal{J}) \le 0$, $\varrho_{1-\varepsilon}\left[\max_{j\in\mathcal{J}}\left[\lambda_j\left(\boldsymbol{X}_j^T\boldsymbol{d} - N_j\right)\right]\right] \le 0$ holds. Thus, proved. □

Appendix C. Scenario-based approach

The scenario-based approach characterizes the random variables by a given set of scenarios. We assume that Θ and d follow a discrete distribution with finite support. Suppose array (θ_{is}, d_{is}) denotes the sth-realization of the expected (daily) demand and the MNCD occurring at site i under scenario $s = 1, \ldots, \mathcal{S}$. For brevity, we assume that the corresponding probability of each scenario is equal (Santoso et al., 2005; Luedtke, 2014).

In light of the non-convexity of joint chance constraints, we introduce big-M constraints (C.3) and (C.4) to replace joint chance constraint (10), where z_s is a binary variable and M is a large positive number. The scenario-based model with a min-max objective is formulated in which the worst case over all scenarios can be considered.

$$\min\ t + \sum_{j\in J}\left\{f_j Y_j + a_j N_j\right\}, \tag{C.1}$$

$$s.t.\ t \ge \beta\sum_{i\in I}\theta_{is}\sum_{j\in J}c_{ij}X_{ijs}, \forall s \in \mathcal{S}, \tag{C.2}$$

$$\sum_{i\in I}d_{is}X_{ijs} - N_j \le Mz_s, \forall j \in J, s \in \mathcal{S}, \tag{C.3}$$

$$\sum_{s\in\mathcal{S}}z_s \le \mathcal{S}(1-\alpha), \tag{C.4}$$

$$\sum_{j\in J}X_{ijs} = 1, \forall i \in I, s \in S, \tag{C.5}$$

$$X_{ijs} \le Y_j, \forall i \in I, \forall j \in J, s \in S, \tag{C.6}$$

$$t \ge 0, X_{ijs} \ge 0, \forall j \in J, s \in S, \tag{C.7}$$

$$z_s \in \{0, 1\}, \forall s \in S, \tag{C.8}$$

$$(4), (5), (6).$$

Constraint (C.2) obtains the maximum cost over all scenarios. Constraints (C.3) together with (C.4) guarantee that the probability of satisfying demands in all scenarios is larger than $1-\varepsilon$: if $z_{jk} = 0$, constraint (C.3) is equivalent to $\Sigma_i d_{ik}X_{ij} \le N_j$; if $z_{jk} = 1$, constraint (C.3) is redundant.

Supplementary material

Supplementary material associated with this article can be found, in the online version, at doi:10.1016/j.trb.2018.11.012.

References

Ahmadi-Javid, A., Seyedi, P., Syam, S.S., 2017. A survey of healthcare facility location. Comput. Oper. Res. 79, 223–263.

ApS, M., 2015. The MOSEK optimization toolbox for MATLAB manual. Version 7.1 (Revision 28).

Ares, J.N., Vries, H.D., Huisman, D., 2016. A column generation approach for locating roadside clinics in africa based on effectiveness and equity. Eur. J. Oper. Res. 254 (3), 1002–1016.

Aringhieri, R., Bruni, M.E., Khodaparasti, S., Essen, J.T.V., 2017. Emergency medical services and beyond: addressing new challenges through a wide literature review. Comput. Oper. Res. 78, 349–368.

Başar, A., Çatay, B., Ünlüyurt, T., 2012. A taxonomy for emergency service station location problem. Optim. Lett. 6 (6), 1–14.

Ball, M.O., Lin, F.L., 1993. A reliability model applied to emergency service vehicle location. Oper. Res. 41 (41), 18–36.

Baron, O., Milner, J., Naseraldin, H., 2011. Facility location: a robust optimization approach. Prod. Oper. Manage. 20 (5), 772–785.

Bayram, V., Tansel, B.c., Yaman, H., 2015. Compromising system and user interests in shelter location and evacuation planning. Transp. Res. Part B 72, 146–163.

Becker, A.B.D., 2011. Decomposition methods for large scale stochastic and robust optimization problems. Massachusetts Institute of Technology. Ph.D. thesis

Bélanger, V., Ruiz, A., Soriano, P., 2019. Recent optimization models and trends in location, relocation, and dispatching of emergency medical vehicles. Eur. J. Oper. Res. 272 (1), 1–23.

Ben-Tal, Nemirovski, 1998. Robust convex optimization. Math. Oper. Res. 23 (4), 769–805.

Ben-Tal, A., Teboulle, M., 1986. Expected utility, penalty functions, and duality in stochastic nonlinear programming. Manage. Sci. 32 (11), 1445–1466.

Beraldi, P., Bruni, M.E., 2009. A probabilistic model applied to emergency service vehicle location. Eur. J. Oper. Res. 196 (1), 323–331.

Beraldi, P., Bruni, M.E., Conforti, D., 2004. Designing robust emergency medical service via stochastic programming. Eur. J. Oper. Res. 158 (1), 183–193.

Bertsimas, D., Sim, M., 2004. The price of robustness. Oper. Res. 52 (1), 35–53.

Bonami, P., Biegler, L.T., Conn, A.R., Cornuójols, G., Grossmann, I.E., Laird, C.D., Lee, J., Lodi, A., Margot, F., Sawaya, N., Wchter, A., 2008. An algorithmic framework for convex mixed integer nonlinear programs. Discrete Optim. 5 (2), 186–204.

Bonami, P., Lejeune, M.A., 2009. An exact solution approach for portfolio optimization problems under stochastic and integer constraints. Oper. Res. 57 (3), 650–670.

Brandeau, M.L., McCoy, J.H., Hupert, N., Holty, J.-E., Bravata, D.M., 2009. Recommendations for modeling disaster responses in public health and medicine: a position paper of the society for medical decision making. Med. Decis. Mak. 29 (4), 438–460.

Çelik, M., Ergun, Ö., Johnson, B., Keskinocak, P., Lorca, Á., Pekgün, P., Swann, J., 2012. Humanitarian Logistics. In: New Directions in Informatics, Optimization, Logistics, and Production. INFORMS, pp. 18–49.

Chang, M., Tseng, Y., Chen, J., 2007. A scenario planning approach for the flood emergency logistics preparation problem under uncertainty. Transp. Res. Part E-logist.Transp. Rev. 43 (6), 737–754.

Chanta, S., Sangsawang, O., 2012. Shelter-site selection during flood disaster. In: Lecture Notes in Management Science, 4, pp. 282–288. Cited By 6

Charnes, A., Cooper, W.W., Symonds, G.H., 1958. Cost horizons and certainty equivalents: an approach to stochastic programming of heating oil. Manage. Sci. 4 (3), 235–263.

Chen, A.Y., Yu, T.Y., 2016. Network based temporary facility location for the emergency medical services considering the disaster induced demand and the transportation infrastructure in disaster response. Transp. Res. Part B 91, 408–423.

Chen, W., Sim, M., 2009. Goal-driven optimization. Oper. Res. 57 (2), 342–357.

Chen, W., Sim, M., Sun, J., Teo, C.P., 2010. From cvar to uncertainty set: implications in joint chance-constrained optimization. Oper. Res. 58 (2), 470–485.

Chen, X., Sim, M., Sun, P., 2007. A robust optimization perspective on stochastic programming. Oper. Res. 55 (6), 1058–1071.

Dalal, J., Üster, H., 2018. Combining worst case and average case considerations in an integrated emergency response network design problem. Transp. Sci. 52 (1), 171–188. doi:10.1287/trsc.2016.0725.

Delage, E., Ye, Y., 2010. Distributionally robust optimization under moment uncertainty with application to data-driven problems. Oper. Res. 58 (3), 595–612.

Döyen, A., Aras, N., Barbarosoğlu, G., 2011. A two-echelon stochastic facility location model for humanitarian relief logistics. Optimization Letters 6 (6), 1123–1145. doi:10.1007/s11590-011-0421-0.

Duran, M.A., Grossmann, I.E., 1987. An outer-approximation algorithm for a class of mixed-integer nonlinear programs. Math. Program. 39 (3). 337–337

Özgün Elçi, Noyan, N., Bülbül, K., 2018. Chance-constrained stochastic programming under variable reliability levels with an application to humanitarian relief network design. Comput. Oper. Res. 96, 91–107.

Elçi, O., Noyan, N., 2018. A chance-constrained two-stage stochastic programming model for humanitarian relief network design. Transp. Res. Part B 108, 55–83. doi:10.1016/j.trb.2017.12.002.

Fan, K., 1972. A minimax inequality and applications. Academic Press, New York.

Fletcher, R., Leyffer, S., 1994. Solving mixed integer nonlinear programs by outer approximation. Math. Program. 66 (1), 327–349.

Gabrel, V., Murat, C., Thiele, A., 2014. Recent advances in robust optimization: an overview. Eur. J. Oper. Res. 235 (3), 471–483.

Galvão, R.D., Morabito, R., 2010. Emergency service systems: the use of the hypercube queueing model in the solution of probabilistic location problems. Int. Trans. Oper. Res. 15 (5), 525–549.

Geroliminis, N., Karlaftis, M.G., Skabardonis, A., 2009. A spatial queuing model for the emergency vehicle distracting and location problem. Transp. Res. Part B Methodol. 43 (7), 798–811.

Ghaoui, L.E., Oustry, F., Lebret, H., 2006. Robust solutions to uncertain semidefinite programs. SIAM J. Optim. 9 (1), 33–52.

Goh, J., Sim, M., 2010. Distributionally robust optimization and its tractable approximations. Oper. Res. 58 (4-part-1), 902–917.

Govindan, K., Fattahi, M., Keyvanshokooh, E., 2017. Supply chain network design under uncertainty: a comprehensive review and future research directions. Eur. J. Oper. Res. 263 (1), 108–141.

Gralla, E., Goentzel, J., Fine, C., 2014. Assessing trade-offs among multiple objectives for humanitarian aid delivery using expert preferences. Prod. Oper. Manage. 23 (6), 978–989.

Hanasusanto, G.A., Roitch, V., Kuhn, D., Wiesemann, W., 2017. Ambiguous joint chance constraints under mean and dispersion information. Oper. Res. 65 (3), 751–767.

He, X., Liu, H.X., 2012. Modeling the day-to-day traffic evolution process after an unexpected network disruption. Transp. Res. Part B 46 (1), 50–71.

Hong, X., Lejeune, M.A., Noyan, N., 2014. Stochastic network design for disaster preparedness. IIE Trans. 47 (4), 329–357.

Horner, M.W., 2008. Testing a flexible geographic information system-based network flow model for routing hurricane disaster relief goods. Transp. Res. Record J.Transp. Res. Board 2022 (2022), 47–54.

Hoyos, M.C., Morales, R.S., Akhavan-Tabatabaei, R., 2015. Or models with stochastic components in disaster operations management: a literature survey. Comput. Ind. Eng. 82, 183–197.

Jia, H., Ordonez, F., Dessouky, M., 2007. A modeling framework for facility location of medical services for large-scale emergencies. IIE Trans. 39 (1), 41–55.

Kınay, O.B., Kara, B.Y., Saldanha-Da-Gama, F., Correia, I., 2018. Modeling the shelter site location problem using chance constraints: a case study for istanbul. Eur. J. Oper. Res. 270 (1), 132–145.

Larson, R.C., 1973. A hypercube queuing model for facility location and redistricting in urban emergency services. Comput. Oper. Res. 1 (1), 67–95.

Larson, R.C., 1975. Approximating the performance of urban emergency service systems. Oper. Res. 23 (5), 845–868.

Lee, T.L., 2008. Back-propagation neural network for the prediction of the short-term storm surge in taichung harbor, taiwan. Eng. Appl. Artif. Intell. 21 (1), 63–72.

Lee, Y.M., Ghosh, S., Ettl, M., 2009. Simulating distribution of emergency relief supplies for disaster response operations. In: Simulation Conference, pp. 2797–2808.

Liberatore, F., Ortuño, M.T., Tirado, G., Vitoriano, B., Scaparra, M.P., 2014. A hierarchical compromise model for the joint optimization of recovery operations and distribution of emergency goods in humanitarian logistics. Comput. Oper. Res. 42, 3–13.
Liu, Y., Li, Z., Liu, J., Patel, H., 2016. A double standard model for allocating limited emergency medical service vehicle resources ensuring service reliability. Transp. Res. Part C 69, 120–133.
Löfberg, J., 2004. Yalmip : a toolbox for modeling and optimization in matlab. In: 2004 IEEE International Conference on Robotics and Automation (IEEE Cat. No.04CH37508), pp. 284–289.
Luedtke, J., 2014. A branch-and-cut decomposition algorithm for solving chance-constrained mathematical programs with finite support. Math. Program. 146 (1), 219–244.
Mak, H.-Y., Rong, Y., Zhang, J., 2015. Appointment scheduling with limited distributional information. Manage. Sci. 61 (2), 316–334.
Meilijson, I., Nádas, A., 1979. Convex majorization with an application to the length of critical paths. J. Appl. Probab. 16 (3), 671–677.
Mete, H.O., Zabinsky, Z.B., 2010. Stochastic optimization of medical supply location and distribution in disaster management. Int. J. Prod. Econ. 126 (1), 76–84.
Ndiaye, M., Alfares, H., 2008. Modeling health care facility location for moving population groups. Comput. Oper. Res. 35 (7), 2154–2161.
Nemirovski, A., Shapiro, A., 2006. Convex approximations of chance constrained programs. SIAM J. Optim. 17 (4), 969–996.
Ni, W., Shu, J., Song, M., 2018. Location and emergency inventory pre-positioning for disaster response operations: min-max robust model and a case study of yushu earthquake. Prod. Oper. Manage. 27 (1), 160–183.
Noyan, N., 2010. Alternate risk measures for emergency medical service system design. Ann. Oper. Res. 181 (1), 559–589.
Noyan, N., 2012. Risk-averse two-stage stochastic programming with an application to disaster management. Comput. Oper. Res. 39 (3), 541–559.
Nurre, S.G., Cavdaroglu, B., Mitchell, J.E., Sharkey, T.C., Wallace, W.A., 2012. Restoring infrastructure systems: an integrated network design and scheduling (inds) problem. Eur. J. Oper. Res. 223 (3), 794–806.
Orgut, I.S., Ivy, J., Uzsoy, R., Wilson, J.R., 2016. Modeling for the equitable and effective distribution of donated food under capacity constraints. IIE Trans. 48 (3), 252–266.
Özdamar, L., Ekinci, E., Küçükyazici, B., 2004. Emergency logistics planning in natural disasters. Ann. Oper. Res. 129 (1–4), 217–245.
Özdamar, L., Ertem, M.A., 2015. Models, solutions and enabling technologies in humanitarian logistics. Eur. J. Oper. Res. 244 (1), 55–65.
Prékopa, A., 1980. Network Planning Using Two-Stage Programming under Uncertainty. Springer Berlin Heidelberg, pp. 1533–1536.
Rawls, C.G., Turnquist, M.A., 2010. Pre-positioning of emergency supplies for disaster response. Transp. Res. Part B 44 (4), 521–534.
Rawls, C.G., Turnquist, M.A., 2011. Pre-positioning planning for emergency response with service quality constraints. OR Spectr. 33 (3), 481–498.
Rockafellar, R.T., Uryasev, S., 2010. Optimization of conditional value-at-risk. J. Risk 29 (1), 1071–1074.
Rottkemper, B., Fischer, K., Blecken, A., Danne, C., 2011. Inventory relocation for overlapping disaster settings in humanitarian operations. OR Spectr. 33 (3), 721–749.
Salmern, J., Apte, A., 2010. Stochastic optimization for natural disaster asset prepositioning. Prod. Oper. Manage. 19 (5), 561–574.
Santoso, T., Ahmed, S., Goetschalckx, M., Shapiro, A., 2005. A stochastic programming approach for supply chain network design under uncertainty. Eur. J. Oper. Res. 167 (1), 96–115.
Scarf, H., Arrow, K., Karlin, S., 1958. A min-max solution of an inventory problem. Stud.Math.Theory of InventoryProd. 10 (2), 201.
Scherrer, C.R., 2008. Optimization of community health center locations and service offerings with statistical need estimation. IIE Trans. 40 (9), 880–892.
Shahabi, M., Unnikrishnan, A., Jafari-Shirazi, E., Boyles, S.D., 2014. A three level location-inventory problem with correlated demand. Transp. Res. Part B 69, 1–18.
Snyder, L.V., 2007. Facility location under uncertainty: a review. IIE Trans. 38 (7), 537–554.
Souza, R.M.D., Morabito, R., Chiyoshi, F.Y., Iannoni, A.P., 2015. Incorporating priorities for waiting customers in the hypercube queuing model with application to an emergency medical service system in Brazil. Eur. J. Oper. Res. 242 (1), 274–285.
Ukkusuri, S.V., Yushimito, W.F., 2008. Location routing approach for the humanitarian prepositioning problem. Transp. Res. Record J.Transp. Res. Board 2089 (6), 18–25.
Wiesemann, W., Kuhn, D., Sim, M., 2014. Distributionally robust convex optimization. Oper. Res. 62 (6), 1358–1376.
Wu, J.D., Li, N., Yang, H.J., Li, C.H., 2008. Risk evaluation of heavy snow disasters using bp artificial neural network: the case of Xilingol in inner Mongolia. Stoch. Environ. Res. Risk Assess. 22 (6), 719–725.
Yang, M., Allen, T.T., Fry, M.J., Kelton, W.D., 2013. The call for equity: simulation optimization models to minimize the range of waiting times. IIE Trans. 45 (7), 781–795.
Yu, L., Yang, H., Miao, L., Zhang, C., 2018. Rollout algorithms for resource allocation in humanitarian logistics. IISE Trans. 0 (0), 1–23.
Yuan, Y., Wang, D., 2009. Path selection model and algorithm for emergency logistics management. Comput.Ind.Eng. 56 (3), 1081–1094.
Zhang, Y., Shen, Z.-J.M., Song, S., 2016. Distributionally robust optimization of two-stage lot-sizing problems. Prod. Oper. Manage. 25 (12), 2116–2131.
Zhang, Z.-H., Berenguer, G., Shen, Z.-J.M., 2015. A capacitated facility location model with bidirectional flows. Transp. Sci. 49 (1), 114–129.
Zhang, Z.H., Jiang, H., 2014. A robust counterpart approach to the bi-objective emergency medical service design problem. Appl. Math. Model. 38 (3), 1033–1040.
Zhang, Z.H., Li, K., 2015. A novel probabilistic formulation for locating and sizing emergency medical service stations. Ann. Oper. Res. 229 (1), 813–835.
Zhang, Z.-H., Unnikrishnan, A., 2016. A coordinated location-inventory problem in closed-loop supply chain. Transp. Res. Part B 89, 127–148.
Zymler, S., Kuhn, D., Rustem, B., 2013. Distributionally robust joint chance constraints with second-order moment information. Math. Program. 137 (1), 167–198.